LUND UNIVERSITY

Master of Science dissertation:

Accuracy of MLC-tracking for inversely optimized arc therapy treatments of varying complexity for two MLCs

Tobias Larsson

Supervisors:
Per Munck af Rosenschöld, Ph. D.
Marianne Falk, M. Sc.
Marianne Aznar, Ph. D.
Stine Korreman, Ph. D.

This work has been performed at the Department of Radiation Oncology, Rigshospitalet, Copenhagen University Hospital, Denmark

Medical Radiation Physics, Clinical Sciences, Lund
Lund University, Sweden, 2010

Acknowledgements

I would like to begin with expressing my gratitude to my supervisors for their dedication and continuous support:

- Thanks to Per for constantly challenging me to perform my very best as well as never forgetting the big picture.
- Thanks to Marianne Falk for her constant guidance and very useful ideas, as well as advice with the practical aspects of my work.
- Thanks to Marianne Aznar for always taking the time to answer my questions and help solve my problems.
- Thanks to Stine for asking the tough questions.

I would also like to thank the research group at Rigshospitalet for their feedback and the medical physicists at Rigshospitalet for their patience when I kept using their equipment.

I would also like to express my gratitude to Varian Medical Systems and the MLC-tracking research group at Stanford for the opportunity to use the MLC-tracking technique in the first place.

Lund, August 16, 2010

Tobias Larsson

Popularized summary in Swedish:

Kompensation av andningsrörelser – nästa steg mot ökad noggrannhet inom strålbehandling?

En mycket vanlig behandlingsteknik vid cancer är strålbehandling. Tekniken har utvecklats snabbt de senaste åren och idag uppnås millimeterprecision för många behandlingsområden. Därmed har behovet av att kunna kompensera för rörelser under behandlingen ökat. I detta arbete undersöktes möjligheten att låta strålgången följa tumören med en teknik som kallas *MLC-tracking*.

Strålbehandling började användas bara något år efter Wilhelm Röntgens upptäckt av röntgenstrålning och har därefter utvecklats till att vara en mycket avancerad behandlingsform. Framförallt de senaste 20 åren har inneburit en enorm utveckling inom området så att röntgenstrålning med hög energi kan riktas mot en tumör med millimeterprecision, samtidigt som bestrålning av frisk vävnad kan undvikas i större och större utsträckning.

Att tumören rör sig under behandlingen är däremot ett problem som fortfarande innebär stora utmaningar. Det är framförallt vid behandling i området kring lungorna som andningen orsakar omfattande tumörrörelser. Lösningen är att ett större område bestrålas, så att strålningen alltid träffas tumören. Nackdelen med detta är att en större del av den friska vävnaden bestrålas och därmed ökar risken för biverkningar.

Kompensation av rörelser

Ett alternativ till att utöka det bestrålade området är att låta strålfältet följa tumören under behandlingen. Detta görs genom att den anordning som formar strålfältet, *flerbladskollimatorn (MLCn),* i realtid justeras efterhand som tumören rör sig. Flerbladskollimatorn består av metallblad som tillsammans formar strålfältet. Tekniken att låta strålningen följa tumören kallas *MLC-tracking* och i detta arbete undersöks hur väl MLC-tracking fungerar för en behandlingsform som kallas *RapidArc*. RapidArc kännetecknas av att bestrålningen sker samtidigt som behandlingsapparaten roterar runt patienten och flerbladskollimatorn formar strålfältet.

Totalt undersöktes 44 olika behandlingsplaner av varierande komplexitet och för två olika typer av flerbladskollimatorer. Resultaten visar att MLC-tracking har potentialen att mycket effektivt kompensera för rörelser, men att prestandan försämras för mer avancerade behandlingsplaner. Resultatet visar också att avstånden mellan bladen i flerbladskollimatorn är avgörande för hur väl tumörrörelser kan kompenseras.

Abstract

Purpose: To investigate the geometric accuracy of MLC-tracking using a circular field, and to investigate the dosimetric accuracy for inversely optimized arc delivery to a moving target. This is done for two different MLCs and for varying plan complexity.

Materials and methods: For investigating the geometric accuracy, a marker was placed on a motion platform while the MLC set to shape a circular field. During tracking of the target, EPID imaging was performed and the geometric accuracy, *i.e.* the difference between the marker and the center of the MLC shape, was calculated for different assumed system latencies. To investigate the dosimetric accuracy, plans were made in Eclipse™ treatment planning system using the RapidArc® treatment technique for two lung cancer patients with a prescribed dose of 2 Gy per fraction. A gantry rotation span of 225° to 135° was used. Four sets of increasingly stringent planning dose objectives (PO) were applied in planning for delivery on a Novalis TX™ linear accelerator (equipped with a High definition MLC (HDMLC)) and on a Varian 2300ix linear accelerator (with the Millennium 120 MLC), for two collimator angles (CA); 45° and 88°. For each patient, one plan was created with CA45 and with an optimization constraint limiting the distance to adjacent leaves. Plans were also created in a clinical version of Eclipse for the PO#1 and PO#2 sets. The number of MU ranged from 334 to 751 for all plans. The plans were delivered to a Delta4® dosimetric device placed on a motion platform moving sinusoidally in the SI direction, with 2.0 cm peak to peak motion and 6 s cycle time. Position monitoring was done using the ExacTrac® optical system. Measurements were made with and without MLC-tracking, and with and without motion. The measurements with a stationary target were used as reference in gamma evaluation, with gamma criteria of 2% and 2 mm (using a dose region of 5-500%). The calculated dose distributions were also used as reference, with gamma criteria of 3% and 3 mm.

Results: For the most suitable assumed latency, the geometric accuracy expressed as RMS value was 0.316 mm and 0.346 mm for the HDMLC and the Millenium MLC respectively. For all RapidArc plans measured, the MLC-tracking method considerably increased the gamma index pass rate for delivery to a moving target compared to delivery with no motion compensation (using the measured dose on a static phantom a reference). The pass rate was also improved for CA 88° compared to 45°. The gamma index pass rate decreased with #MU for both MLCs with CA 45°. Dose profile analyses showed that overdosage in the high dose region was the primary cause of gamma evaluation failures. The pass rate was significantly higher (P=0.0025) for measurements using the Millennium MLC compared to the HDMLC. A correlation was seen between reduced average adjacent leaf distance (weighted against the dose weight for the corresponding control point) and improved gamma index pass rate.

Conclusion: It is possible to use MLC-tracking during RapidArc® delivery to compensate for the target motion simulated in this study. The gamma index pass rate was increased using MLC-tracking, but the effect tended to decrease slightly for the more complex plans. Aligning the leaves with the target motion substantially increased the gamma index pass rate for both MLCs, regardless of the plan complexity. The distance to adjacent MLC leaves seems to be an important factor in predicting MLC-tracking performance.

Abbreviations and acronyms

3DCRT	Three dimensional conformal radiotherapy
AAA	Analytical anisotropic algorithm
ALDw	Weighted average adjacent leaf distance
AP	Anterior-posterior
BEV	Beam's eve-view
CT	Computed tomography
DVH	Dose-volume histogram
HDMLC	High definition MLC
HI	Heterogeneity index
IMAT	Intensity modulated arc therapy
IMRT	Intensity modulated radiotherapy
Linac	Linear accelerator
LR	Left-right
M-MLC	Millennium MLC
MLC	Multileaf collimator
MRDC	Multi-resolution dose calculation algorithm
MU	Monitor units
OAR	Organ at risk
RMS	Root mean square
PRO	Progressive resolution optimizer
PTV	Planning target volume
PVI	Portal Vision Imaging
SI	Superior-inferior
SSD	Source-skin distance
TPS	Treatment planning system
VMAT	Volumetric modulated arc therapy

Table of contents

1 Introduction

The aim of radiotherapy is to deliver a high enough radiation dose to a cancer tumour so that its growth is permanently halted and the metastatic spread stopped, while the dose to healthy organs is limited. In areas of the body where the tumour moves during a radiation treatment this objective becomes more difficult to accomplish since additional margins are required to guarantee tumour coverage. There are however techniques that limits the effect of the motion; two of these are gating and MLC-tracking [1]. MLC-tracking is a method in which the shape of the MLC follows the projection of the target volume. This study investigates the accuracy of MLC-tracking for inversely optimized arc therapy deliveries, using the RapidArc treatment technique, of treatment plans of varying complexity for two different MLCs.

1.1 Aim

The aim of this study is to investigate the geometric accuracy of the MLC-tracking technique and its dosimetric accuracy for RapidArc treatments, as well as to derive a patient independent parameter to predict the performance of the tracking system. As the MLC-tracking technique uses input from an external position system, the BrainLab ExacTrac monitoring system in this case, the performance of this system is also investigated.

The geometric accuracy is investigated by continuous imaging of the MLC and a marker that is tracked by the MLC-tracking system. The dosimetric accuracy is investigated with a diode array, the ScandiDos Delta4, and the gamma evaluation method is used for comparison of treatments delivered with and without tracking, and with and without a moving target.

As RapidArc treatments can show a large variety in complexity [2], the performance of the MLC-tracking system is expected to vary with different plan. A parameter that predicts the MLC-tracking performance based on the shape of the MLC is derived. As the choice of collimator angle with regard to the target motion may also be of importance [3], this is also investigated using two different collimator angles.

1.2 RapidArc

RapidArc is a commercial product for intensity modulated rotational radiotherapy from Varian (Varian Medical Systems, Palo Alto, California, USA). It uses a gantry rotation span during which the dose rate and gantry speed as well as the shape of the MLC are varied in order to create conformal dose distributions.

1.2.1 Background

Intensity-modulated radiation therapy (IMRT) is an umbrella term for radiotherapy treatment techniques that modulates the intensity of the radiation to create conformal dose distributions. The principle can be traced back to publications by Brahme et al. in 1982 and 1988 [4, 5]. IMRT differ from traditional conformal radiotherapy (3DCRT) since several non-uniform two-dimensional intensity profiles are used to create conformal dose distributions, as well as the desired fluence being inversely optimized. The dose distribution can for example be made to encompass a tumour while keeping the dose to nearby organs at risk at a minimum and even to deliver a uniform dose to a tumour that encircles a risk organ.

The traditional implementation of IMRT (here called fixed-beam IMRT) uses a set of fixed gantry angles and modulates the beam fluence with the MLC. Typically, one distinguishes between two methods of delivery; sliding window (or dynamic) IMRT and step-and-shoot IMRT. Both variants have in common that the treatment takes up to 10 minutes [6].

1.2.2 Arc therapy

A different approach to create a conformal dose distribution was taken by Yu et al. [7] in 1995 with a technique called IMAT (intensity modulated arc therapy) which uses several superimposed arcs in which the gantry continuously rotates during irradiation and the MLC changes shape between so-called control points [7, 8]. IMAT was limited by the fact that several arcs (two to five according to the 2003 publication) were needed to achieve complex dose distributions and the advantage compared to fixed-beam IMRT with regards to treatment time was therefore not decisive.

In 2008 Otto [9] further developed arc therapy by introducing a new optimization method that allowed for varying the MLC shape as well as the gantry rotation speed and the dose rate. This enabled the number of arcs to be reduced to one while maintaining a conformal dose distribution (although the option for several arcs was maintained). The optimization method uses control points and resolution levels. Each control point corresponds to a certain MLC shape and gantry angle, and a dose weight that describes the number of monitor units required. Linear interpolation is used to define the motion of the MLC leaves between adjacent control points. Resolution levels are used in the sense that at the first level, widely separated control points, allowing large differences in the MLC shapes, are utilized for a course optimization. The resolution level is then increased by adding control points between existing ones, so that the number of control points is (approximately) doubled. The process continues until the preferred number of control points has been reached, usually one to two control points per gantry angle degree. The technique was named VMAT (volumetric modulated arch therapy), and was commercially implemented when Varian released RapidArc.

The objective of VMAT is to deliver a radiation dose of high conformity with a high degree of efficiency [9], which compared to "standard" IMRT means a shorter treatment time and the use of fewer monitor units while still obtaining similar or improved dose distributions. A shorter treatment time reduces the risk of unexpected intrafractional organ motion, decreases the patients discomfort and increases patient throughput. Treatment times in the order of 1-2 min for a 2 Gy fraction dose have been reported [10]. The use of fewer monitor units results in a reduced body dose from leakage radiation which may decrease the risk of secondary malignancies [11]. There may also be a radiobiological advantage as investigated by [12] in delivering the entire radiation dose is a short time span, for example when comparing RapidArc to fixed-beam IMRT.

1.2.3 Clinical implementation of RapidArc

RapidArc was clinically released in April 2008 and the first clinical implementation was treatment of prostate cancer, with the first treatment at this hospital carried out in May 2008 [13]. RapidArc has since found a wider clinical acceptance and its use has been investigated for a number of treatment sites, including prostate, brain, H&N, gynecological and lung treatments [10, 14-19]. Generally, the dose distributions achievable with RapidArc have been better or equal to those realizable with fixed-beam IMRT [10, 14-19].

1.2.4 Optimization and dose calculation

RapidArc treatment planning in Eclipse, Varian's treatment planning system (TPS), is similar to IMRT treatment planning with the differences that a treatment arc spanning a range of gantry angles is created and that resolution levels are used in the optimization process. The option to use multiple arcs is also available. Dose objectives are set for the PTV and OARs, and dose differences between the objectives and the calculated dose are used in an objective function. The aim of the iterative process is to minimize the objective function, as in planning of fixed-beam IMRT.

For RapidArc, the dose distribution is calculated with the Analytical Anisotropic Algorithm (AAA), which is a pencil-beam, convolution-superposition model. It uses a data from Monte Carlo simulations that are adjusted based on measurements and allows for inhomogenity corrections based on scaling of photon and electron scatter kernels [20].

Dose calculations for RapidArc treatments of lung presents special challenges for the calculation algorithm used (not considering tumour motion). The challenge is twofold; (1) the often complicated shape of the MLC and (2) the density variations in or near the target. For a RapidArc treatment, the MLC-shapes for a single control point may be very complicated with the open field sometimes defined by a single leaf with neighboring leaves closed, or the opposite case with a single closed leaf next to several leaves that are open. See Figure 1 for an example taken from this study. It has been shown that the dose calculated with the AAA deviates from Monte Carlo simulations for these situations, as well as near the

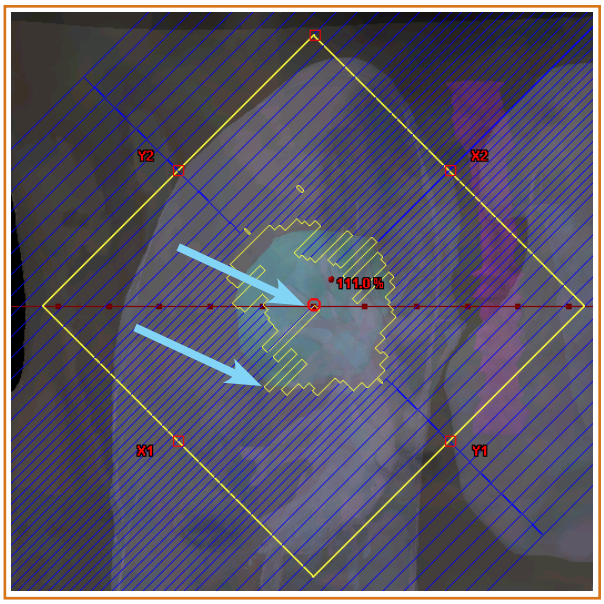

Figure 1. An example of a MLC-shape with leaf configurations that is difficult for dose calculation algorithms to handle correctly (arrows).

leaf tip [21]. The second challenge is the density variations in the lung. The change in density in the transition between the lung tissue and solid tissue, such as the tumour or adjacent bone, causes a build-up effect. Several studies have also shown the problem for calculation algorithms to account for lateral density variations, for example [22] and [23], although the AAA was found to perform adequately.

In the optimization process of a RapidArc treatment, the progressive resolution optimizer (PRO) uses a fast and less accurate dose calculation algorithm (i.e. the "Multi-resolution dose calculation", MRDC). The algorithm is used for a quick dose estimation and the dose calculation is therefore not as accurate as using the AAA [20]. For example, large differences in for example PTV coverage can be seen for lung treatments when comparing the DVH from the optimization with the DVH after the AAA dose calculation. To address this problem, a feature is available in a research version of Eclipse that uses the dose distribution calculated with the AAA for a base for an additional optimization. This feature was used in creating some of the plans used in this study, see Section 2.1.2.

1.3 Lung cancer

Lung cancer is a type of cancer originating in the lungs that is characterized by treatment challenges and, generally, bad prognoses. In this section a brief overview is given of its incidence and mortality, the treatment options and the tumour motion associated with treatments of lung cancer in radiotherapy.

Although lung cancer is only the fifth most common form of cancer in Sweden, with an incidence of about 35 cases per 100 000 inhabitants, it causes the most cancer-related deaths [24]. The 5-year survival is about 12% for men and 15% for women, making it one of the cancer types with the worst prognosis [24]. Treatment options include surgery, and radio- and/or chemotherapy. For inoperable tumours, which occur in about two thirds of the cases, radio- or chemotherapy, or both, are the treatment options. Studies have shown that increasing the radiation dose to the tumour may have a positive impact on the local control, and a new treatment paradigm has emerged that uses high fraction doses and accurate patient set up, commonly referred to as stereotactic body radiation therapy [25, 26].

Treating lung cancer with radiotherapy is especially challenging due to the tumour motion associated with breathing. It has been shown that the motion occurs primarily in the superior-inferior direction, and motion amplitudes as large as 2.5 cm have been observed [27]. When the target (i.e. the tumour) is moving during radiotherapy, two effects cause the delivered dose to differ from the planned dose; dose blurring and interplay effect. These are explained below.

Dose blurring (or "dose smearing") is a direct effect of tumour motion: as the tumour moves, the resulting dose distribution will be smeared out compared to the dose distribution for a static target. The clinical solution for this effect is to either use larger margins, or to take the dose blurring into account in the treatment planning [1, 28]. Any degradation of the treatment with regards to target coverage can

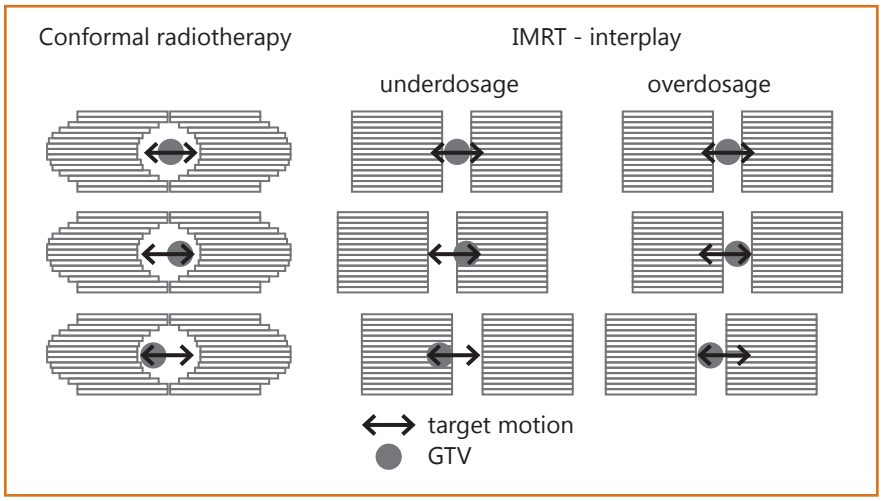

Figure 2. Illustration of the interplay effect which can be exemplified as interference between the linac and the target.

thereby be compensated, at the expense of a higher dose to the healthy tissue. Guckenberger et al. found that for a motion amplitude of 2.0 cm, the margins in the superior-inferior direction would have to be increased by 6 mm to ensure complete CTV coverage. By accepting a 5% dose loss to the CTV would be acceptable, the margin increase would be limited to 3.5 mm [28]. Previous works with MLC-tracking has shown that the technique is capable of reducing the necessary margins [3].

The interplay effect is the effect that may occur as the motion of the linac (primarily the MLC) and motion of the target interferes, and causes unwanted dosimetric effects. As dose blurring occurs regardless of the treatment technique, the interplay effect is limited to intensity modulated treatments, where only a fraction of the PTV is irradiated at any given time. A simple example of the effect is illustrated in Figure 2.

The interplay effect has been investigated for both dynamic IMRT [29] and for RapidArc [2]. For dynamic IMRT, Court et al. found that for many target motion patterns, the speed of the MLC would need to be decreased to approximately a third of its standard value in order to keep the dose deviation caused by the interplay effect at less than 10% for each fraction [29]. For RapidArc treatments, the interplay effect was found to be dependent on the motion pattern, with a larger effect with larger amplitudes and with longer cycle times. It also increased with the number of monitor units used for the treatment. For one case, 87% of the target volume got more than 3% dose error. The dose error was however less than 10% for 98% of the target volume, for all the cases investigated [2]. The interplay effect is likely to average out over many fractions, but that may not be the case for hypofractionated treatments such as stereotactic radiotherapy due to the small number of fractions delivered [1].

The use of MLC-tracking has the potential to decrease the impact of both these effects since the aim of MLC-tracking is to geometrically compensate for the target motion.

1.4 MLC-tracking

MLC-tracking is a pre-clinical motion compensation technique that changes the shape of the MLC based on the motion of the tumour. In this study, tracking algorithms first described by Sawant et al. [30] are used. Previous studies where MLC-tracking was used during RapidArc treatments have shown both its feasibility [31], and the effect of different amplitudes of motion [3]. This study expands upon previous studies by comparing RapidArc plans of different complexity, as well as studying MLC-tracking for different MLCs. It shall be noted that the MLC-tracking software is under development and that the technique as such is not commercially available. Publications from other groups have investigated the dosimetric advantages of using a tracking technique [32] as well as dynamic MLC-tracking for Siemens linear accelerators [33].

The MLC-tracking uses real-time information of the tumours location obtained from an external monitoring system such as kV- and or MV-imaging of internal markers or internal structures [34, 35], optical information of external markers [3, 30, 31, 36] or internal transponders [37]. In this study, positional information is obtained by optical imaging of external markers using the BrainLAB (BrainLAB AG, Heimstetten, Germany) ExacTrac monitoring system. The MLC-tracking system uses the information to calculate a new MLC shapes to compensate for the recorded motion.

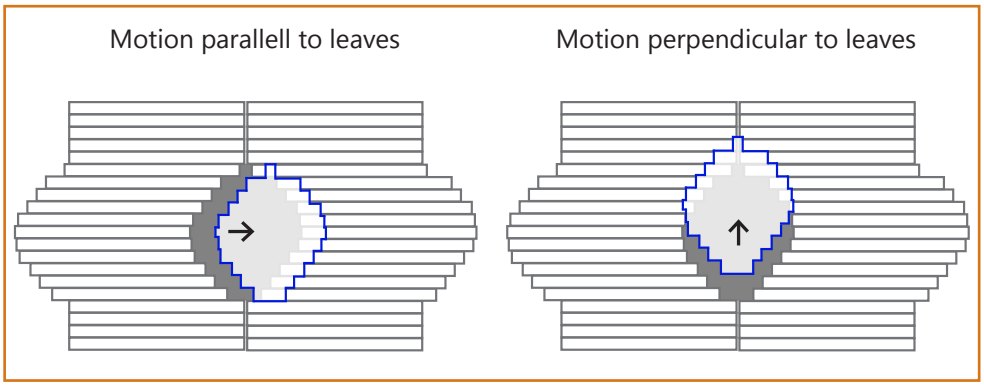

Figure 3. The two kinds of MLC motion compensation, for motion parallel as well as perpendicular to the MLC leaves travelling direction. The arrow illustrates the direction and amplitude of the target motion.

It has been shown that the tracking error is larger and that the efficiency is lower when the target motion is perpendicular to the travel direction of the MLC leaves, compared to parallel motion [30] (Figure 3). This is caused by the motion requiring the MLC leaves to shift position, which, depending on the MLC shape, might require a leaf to travel a distance that is too long for it to be able to achieve the new position quickly enough. Motion parallel to the MLC leaves on the other hand only cause the leaves to move short distances, in association with the target movement.

1.4.1 Principle

The MLC-tracking system requires a data file containing the MLC shapes for the treatment, for a RapidArc plan the file contains the MLC shapes for each control point and the corresponding gantry angle. The planned MLC shape is transformed to compensate for translation (target deformation and rotation could in theory also be accounted for) and new leaf positions are calculated. The process is described below.

1. Planned MLC shapes are extracted from the planned leaf positions for each control point, which are read from a data file (called .MLC-file) and linearly interpolated between adjacent control points.

2. The target position obtained from the external monitoring system is transformed from the treatment room reference system to the BEV reference system.

3. To compensate for the latency in the whole system, a prediction algorithm is used to calculate the expected future position of the target. Based on the targets position, the algorithm predicts the expected position with a time difference that is equal to the assumed latency.

4. The planned MLC shape is transformed into a new MLC shape that compensates for the target motion. This is a purely geometric transformation so influences from tissue inhomogeneities and off-axis effects are ignored.

5. New leaf positions are calculated from the desired MLC shape. The new MLC positions are sent to the MLC-controller and the MLC leaves moved accordingly.

As the jaws are set wider than usually when using MLC-tracking (see Section 2.1.5), leaf pairs that are not needed for tracking are moved to the side, so that the opening between the opposing leaves are screened by the jaws. This is done to avoid unnecessary irradiation. However, unused leafs that are the closest to open leafs are kept centered and ready to be used should the target move in that direction. The number of adjacent leaves that are kept at the center can be selected in the MLC-tracking software from two to five.

1.4.2 Latency

The latency of the MLC-tracking system is the time delay from when a positional change occurs and when the MLC compensates for the motion (i.e. when the new, correct, position has been reached) [36]. It has been shown that the latency is an important source of error in current implementations of MLC-tracking [36, 38], and efforts have been made to predict the expected location of a tumour based on its motion [38]. In this study a motion prediction algorithm was employed that used position data collected several seconds prior to predicting the position.

The latency in the MLC-tracking system originates in several sources; (1) the sampling frequency of the monitoring system, (2) the time of averaging in the monitoring system, (3) network limitations, (4) cal-

culation of new MLC positions and (5) response time of the MLC for these new positions. Previous studies have measured the latency of the MLC-tracking system various monitoring systems. Using the Varian RPM, a latency of approximately 160 ms has been reported [3, 30, 31]. With the Calypso implanted electromagnetic transponder (Calypso Medical Technologies, Seattle, WA, USA), the latency was measured to be about 220 ms [37]. Using the kV imager attached to the linac, the latency was measured to be 570 ms with 5 Hz imaging [35]. The latency was measured for the MLC-tracking system using ExacTrac for monitoring as a part of this study.

1.5 Gamma evaluation

The gamma method is a comparison method introduced by Low et al. [39, 40] as a quantitative measurement of difference between the two dose distributions, an evaluated (e.g. a measured dose distribution) and a reference (e.g. a calculated dose distribution). It combines the use of calculating the dose difference (i.e. dose deviation) for each reference point with the spatial distance to where the same dose is found (i.e. distance to agreement, DTA). In other words, the comparison is carried out both in the quantities of dose and space.

To only use dose deviation or distance to agreement has its drawback, as the two methods each has its disadvantages; the dose deviation is sensitive to spatial differences in areas of large dose gradients and the distance to agreement is susceptible to small dose differences in low dose regions. The gamma evaluation enables to distance to agreement to be the primary method in areas where the dose deviation fails, and vice versa.

In performing the gamma evaluation, a generalised gamma function is calculated for all reference points, as follows:

$$\Gamma\left(\mathbf{r_e}, \mathbf{r_r}\right) = \sqrt{\frac{r^2\left(\mathbf{r_e}, \mathbf{r_r}\right)}{\Delta d^2} + \frac{\delta^2(\mathbf{r_e}, \mathbf{r_r})}{\Delta D^2}} \qquad (1)$$

where $\mathbf{r}_e$ is the evaluated position, $\mathbf{r}_r$ is the reference position, $r(\mathbf{r}_e, \mathbf{r}_r)$ is the spatial distance between the evaluated and the reference position, $\delta(\mathbf{r}_e, \mathbf{r}_r)$ is the difference between the evaluated dose at position $\mathbf{r}_e$ and the reference dose at position $\mathbf{r}_r$, Δd^2 is the distance to agreement criterion (e.g. 3 mm), and ΔD^2 is the dose deviation criterion (e.g. 3%).

After obtaining the generalised gamma function, the minimum generalised gamma function $\gamma(\mathbf{r}_r)$ is calculated by

$$\gamma(\mathbf{r_r}) = \min\left\{\Gamma(\mathbf{r_e}, \mathbf{r_r})\right\} \forall \left\{\mathbf{r_r}\right\} \qquad (2)$$

The right hand side of Equation 2 above is the maximum distance in the dose and distance reference system that is allowed for the evaluation to pass, the evaluation therefore passes if $\gamma(\mathbf{r}_r) \leq 1$, and fails if $\gamma(\mathbf{r}_r) > 1$. The term "gamma pass rate" is the percentage of the evaluated positions that passes the evaluation, for a specific combination of a measured and an evaluated dose distribution. In this study, the gamma evaluation tool implemented in the Delta4 software (Section 2.2.2) is used to calculate the gamma index pass rate.

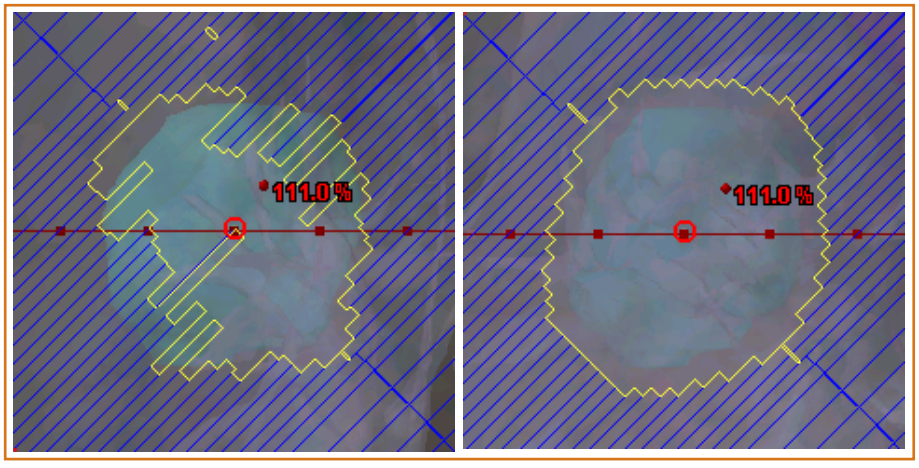

Figure 4. A complex (left) and simple (right) MLC shape, showing the qualitative difference that is easy to distinguish but somewhat more difficult to quantify. An attempt to do this is to use the adjacent leaf distance, see Section 2.1.3.

1.6 Plan complexity

When “plan complexity” is used in the literature, it sometimes refers to the number of segments or monitor units used in an IMRT treatment plan, e.g. in [41]. In the article by Court et al. [2], “plan complexity” is directly related to the number of monitor units used in a RapidArc treatment. Therefore, for relative and qualitative measurement of plan complexity, the number of monitor units needed to deliver a certain dose may be used. However, the number of monitor units is a parameter that does not describe the underlying plan properties that make a plan complex. To the authors knowledge, no publication has proposed parameters that accurately quantifies the complexity of RapidArc treatments. In this study, the average distance between adjacent MLC leafs is used as a quantification of the MLC complexity from a MLC-tracking perspective, see Section 2.1.3.

The term plan complexity is used to describe how complicated a RapidArc plan is to deliver. A more modulated plan would be more complicated than a less modulated plan, as the number of monitor units would tend to be higher, the MLC leaves would move more often and the MLC generally exhibit more complicated shapes. The gantry speed would be reduced as the number of monitor units per gantry angle would be increased becuase of the maximum dose rate being insufficient. It is plausible that a complex plan put greater requirements on the linear accelerator and that the quality of the delivery might decrease. The accuracy of the dose calculation is also expected to decrease for more complex MLC shapes (Section 1.2.4).

Plan complexity is relevant when MLC-tracking is used in the sense that the MLC leaves will be used for modulation a larger fraction of the time for a more modulated plan when compared to a less modulated plan. As motion that is not parallel to the leafs traveling direction requires for the MLC leaves to adapt the position of its closet neighbor, a complicated MLC shape with large distance between MLC leaves is expected to be more challenging for MLC-tracking than a simpler shape (e.g. resembling a circle). The MLC shapes for two control points from the same RapidArc treatment may show quite different shapes (Figure 4).

2 Materials and methods

2.1 Treatment planning

To evaluate the accuracy in RapidArc deliveries with MLC-tracking for different plan complexity, two patients were selected and several treatment plans were created for each patient. The objectives were defined so that different plans showed a range of complexities; from very simple to very complex plans, as well as those realistic for clinical application.

In order to evaluate the difference in MLC-tracking dosimetric accuracy when the leaves are aligned to the motion of the target, plans were also created with a collimator angle of 88°. A collimator angle of 90° aligns the leaves perfectly to motion in the superior-inferior direction but would be avoided clinically since the interleaf leakage would irradiate the same volume of the patient, similarly to using a collimator angle of 0° in fixed-beam IMRT. This effect would be increased when using MLC-tracking as a wider jaw setting is required (Section 2.1.5). It has been shown that a collimator angle of 90° gives worse optimization results than 45° in treatment planning of RapidArc plans, although the difference found was not statistically significant [42]. The potential benefit with MLC-tracking and a collimator angle of 88° compared to 45° would therefore have to be investigated with regard to clinical use.

For the collimator settings of 45°, treatment plans were created in both a research version of Eclipse, as well as the clinical version used at Rigshospitalet (version 8.6). The research version allowed for further variation in plan complexity. For each patient and MLC type, a plan was also created using an additional hardware constraint in the optimization; restricting the distance between adjacent MLC leaves. A treatment plan using this constraint was expected to be more suitable for MLC-tracking since the risk of a leaf having to travel too far to be able to compensate for the target motion would be decreased.

2.1.1 Patient cases

From the patient material available at Rigshospitalet, two patients treated for lung cancer were selected to be used in this study. They were chosen based on the tumours location and size (relatively small targets were preferred to emphasize the effect of motion compensation). For the two patients a dose of 2 Gy per fraction was used during the entire study, normalized to 100% at target mean. See Table 1 for details. For both patients, the OARs were the left and right lung and the spinal cord.

2.1.2 Creating and optimizing RapidArc treatment plans

For each patient four sets of increasingly stringent planning objectives were created. All the sets had in common that the gantry angles spanned 270°, from 225° to 135°. The planning objectives for the target volume was consistently kept at PTV_{min} = 98.4% and PTV_{max} = 101.5% of the prescribed dose except for the first set where PTV_{min} = 94.5% and PTV_{max} = 104.5% were used. The objectives for the OARs and the use of a monitor unit objective function differed between the sets, as described below. In order to avoid dose deposition close to but outside of the target volume, a dose constraint was employed for an additional structure that was based on the PTV but with a margin of 0.4 cm and reaching 3 cm further outside of the target volume.

- **Planning objective set #1**. With very loose dose objectives for OARs, the cost function only comprised the PTV objectives. A tight MU objective was used with a maximum number of MUs of 300, which even though it was an unrealistic restriction, it kept the number of MUs and thus the complexity as low as possible.

Table 1. PTV information for the two patients used in this study.

	Target location	PTV dimensions (cm)			PTV volume (cm³)
		AP	SI	LR	
Patient A	Upper right lobe	4.4	5.3	4.9	60.96
Patient B	Near the mediastinum, superior to the heart	4.8	2.6	4.3	22.67

- **Planning objective set #2**. This set used with objectives so that the optimization became a compromise between PTV coverage and sparing of the OARs. Although a MU objective of maximally 600 MU was used it had a minor impact on the optimization, showed by the fact that the MU restriction was not reached (the plan with the highest number of MUs used 570 MUs). These plans would likely be a clinically feasible with regards to number of monitor units and doses to the OARs.

- **Planning objective set #3**. These plans were created with similar objectives as set #2, with the added use of the Eclipse research version feature allowing reoptimization based on the AAA-calculated dose distribution. For the plans using a constraint on the distance to adjacent MLC leaves, no MU objective was used.

- **Planning objective set #4**. This set used tougher planning objectives compared to planning set #3 for the OARs as well as a higher penalty for under- and overdosage to the PTV. By not using a MU objective, the optimizer was allowed to unimpededly increase the plan complexity. In creating these plans, the same research feature was used as in set #3.

For each patient, the plans were first optimized and calculated for the Novalis TX treatment unit (with the HDMLC) and thereafter for delivery on a Clinac 2300ix (with the Millennium 120 MLC (M-MLC)). Because of the stochastic nature of the optimization process [6] and the different hardware prerequisites, plans created with the same set of planning objectives were different with regards to the number of monitor units and the resulting dose distributions. See Table 2 for common properties for the plans, and Table 3 for plan details.

2.1.3 Evaluation of the treatment plans

As measurements of the plan complexity, two parameters were used. The first is the number of monitor units (#MU). Since all plans used the same prescribed dose and gantry span, a higher number of monitor units roughly corresponded to a smaller area of the PTV being irradiated at any given time, thus increasing the modulation and the complexity of the plan.

As a measure of the challenge a plan presents for MLC-tracking, the weighted average adjacent leaf distance, ALD_w, is introduced. This is the average adjacent leafs distance for all control points, obtained by averaging the average adjacent leaf distance for each control point weighted against the dose weigh, which is the parameter that defines the number of monitor units that is to be given for each control point in the delivery (it is normalized here so that the average value of all dose weights equals 1). The weighted average adjacent leaf distance is mathematically expressed as follows:

$$ALD_w = \frac{1}{n}\sum_{i=1}^{n} d_i \cdot w_i \qquad (3)$$

where d_i is the mean adjacent leaf distance for control point i, and w_i is the normalized dose weight for control point i and n is the number of control points. The mean adjacent leaf distance for each control point is calculated by:

Table 2. Common properties of the treatment plans.

	Treatment technique	Gantry span	Jaws setting	Dose calculation grid size	Treatment optimization algorithm		Dose calculation algorithm	
					Research TPS	Clinical TPS	Research TPS	Clinical TPS
Patient A	RapidArc	225°-135°	13 cm × 13 cm	0.25 cm	PRO 9.0.5	PRO 8.6.15	AAA 10.0.1	AAA 8.6.15
Patient B	RapidArc	225°-135°	8 cm × 8 cm	0.25 cm	PRO 9.0.5	PRO 8.6.15	AAA 10.0.1	AAA 8.6.15

Table 3. Plans created for Patient A and B.

Plan number	Collimator angle (°)	TPS and special remarks	Planning objective set	#MU (HDMLC / M-MLC)	
				Patient A	Patient B
01	45	Research TPS	PO #1	352 / 350	417 / 393
02	45	Research TPS	PO #2	508 / 486	544 / 494
03	45	Research TPS, reopt.†	PO #3	516 / 518	582 / 527
04	45	Research TPS, reopt.†	PO #4	701 / 686	555 / 545
05	88	Research TPS	PO #1	382 / 403	480 / 460
06	88	Research TPS	PO #2	478 / 482	540 / 524
07	88	Research TPS, reopt.†	PO #3	499 / 451	570 / 502
08	88	Research TPS, reopt.†	PO #4	684 / 523	546 / 569
09	45	Clinical TPS	PO #1	334 / 334	400 / 393
10	45	Clinical TPS	PO #2	577 / 579	559 / 438
11	45	Research TPS, reopt.†, distance constraint*	PO #3	751 / 723	648 / 673

†: for these plans, the final dose calculation was used for an additional optimization
*: for these plans, a constraint for the distance to adjacent MLC leaves was applied in the optimization process

$$d = \frac{1}{N}\sum_{j}^{N}\frac{(|x_j - x_{j-1}| + |x_j - x_{j+1}|)}{2} \quad (4)$$

where x_j is the position for leaf j and N is the number of open leafs for the specific control point.

2.1.4 Creation of verification plans

For the clinical quality control of RapidArc treatments with the Delta4 (the dosimetric phantom used in this study (Section 2.2.2), verification plans were created in Eclipse. In order to do this, the Delta4 phantom was modeled as a cylinder with the HU-value corresponding to the PMMA of the phantom. This model of the phantom was used instead of an actual CT scan to avoid attenuation artifacts from the diodes.

As MLC-tracking experiments were done with the Delta4 placed on top of the motion platform, the motion platform had to be included as well. The platform was therefore modeled as a parallelepiped with the correct dimensions and with a HU-value of 108 (based on previous transmission measurements with an ionization chamber). In order to decrease the impact of uncertainties in modeling of the platform and the couch when comparing measurements with calculated doses, the gantry span used for the treatments was chosen so that both the treatment couch and the motion platform were almost entirely avoided (Figure 5).

When preparing a treatment plan for verification, the treatment is applied to the verification structure set with the center of the Delta4 phantom placed at the isocenter. The dose is then calculated and the resulting dose distribution as well as the treatment plan is imported into the Delta4 software allowing comparison with the measured dose.

2.1.5 Adapting plans for MLC-tracking

When treatment plans are to be used for MLC-tracking, the jaws are set differently than for a standard RapidArc treatment. For a standard treatment, the jaws are set as close to shape of the PTV as possible so that unused leaf pairs are shielded by the jaws and leakage radiation is avoided. When using MLC-tracking, since the shape of the MLC will follow the motion of the target, the jaws have to be set wider. If the amplitude of the motion is known, the jaws can easily be set to encompass the maximum expected target displacement. If anomalously large motion occurs, causing the target to move underneath the jaws, the MLC-tracking software assets beam-hold.

In order to set the MLC carriages outside of the jaws, so that the leaves can move in the entire area defined by the jaws, the positions of the first leaf pairs are manually set to 0.5 cm wider than the jaws for the first control point. For the subsequent control points, the leaf pair is gradually closed. Since the first leaf pair is located at the very periphery of the MLC, it is completely covered by the jaws and does not affect the treatment.

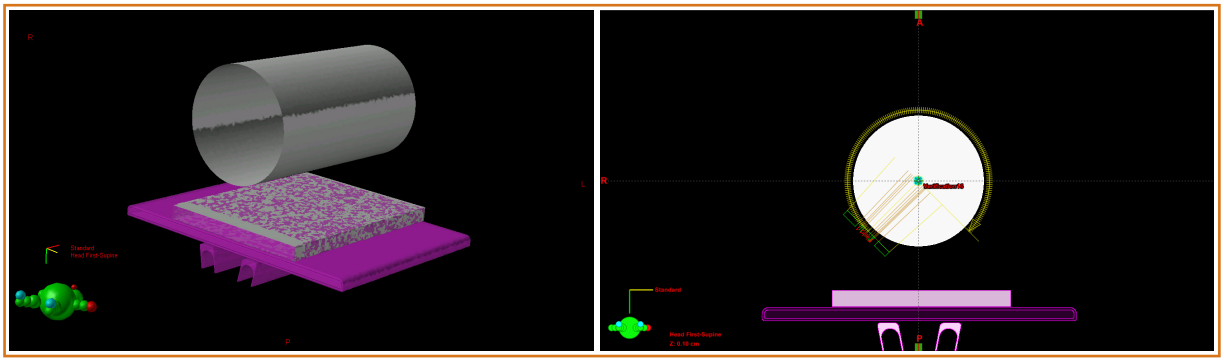

Figure 5. Two views of the verification sets in Eclipse, a 3D view of the cylinder and couch with the motion platform (left) and a transversal view also showing the gantry span used for the treatment plans (right).

As the MLC-tracking software requires the MLC positions for the control points in the treatment, these are exported separately from Eclipse to an .MLC-file. The file contains patient information, the type of treatment (e.g. RapidArc), the MLC model and the leaves positions for each control point as well as the gantry angle for each control point. In order to export this file from Eclipse, the gantry angle for each control point is set to zero. This information is therefore restored using a simple MATLAB program.

2.2 RapidArc measurements

2.2.1 The HDMLC and the Millennium 120 MLC

In this study, MLC-tracking was investigated for two MLCs; The Millennium 120 MLC (M-MLC) and the HD120 MLC (HDMLC). The M-MLC has 60 leaf pairs of two leaf widths; the central 40 leaf pairs have a width of 5.0 mm and the peripheral 20 have a leaf width of 10.0 mm (projected at isocenter). The HDMLC has in contrast 32 central leaf pairs with a leaf width of 2.5 mm and 28 peripheral leaf pairs with a width of 5.0 mm (Figure 6). The central 8 cm of the MLC has therefore twice as high resolution, making it possible to create MLC shapes that better approximates the PTV projection. The HDMLC is also characterized by a sharper penumbra and reduced leakage radiation when compared to the M-MLC [43-45].

It has been shown in treatment planning studies that using the HDMLC can create better dose distributions than using the Millennium MLC, finding significant differences in both target coverage and OAR sparing for some cases and non-significant differences in some cases [11, 43, 46]. In a theoretical study, Bortfeld et al. found that for a 6 MV beam in soft tissue, the optimal leaf width is in the order of 1.5-2 mm, thus giving a theoretical justification to use a leaf width of 2.5 mm [47].

2.2.2 The Delta4 dosimetry phantom

In order to investigate the dosimetric accuracy in the delivery of RapidArc plans with MLC-tracking, the Delta4 (ScandiDos, Uppsala, Sweden) dosimetry phantom was used. The Delta4 contains 1069 cylindrical p-Si diodes with a diameter of 0.5 mm, a height of 0.05 mm and an effective volume of 0.78 mm^3. The diodes are arranged in two (almost) perpendicular arrays, each array covering an area of 20 cm × 20 cm, with the diodes separated by 0.5 cm in the central 6 cm × 6 cm, and 1.0 cm in the peripheral part. The arrays are enclosed by a cylindrical phantom with 22 cm in diameter and 40 cm in length, made of Polymethylmethacrylate (PMMA) with a density of 1.19 g cm^{-3}.

The proprietary evaluation software allows for evaluation of measured dose distributions with both planned and other measured dose distributions. When comparison is made with a planned dose distribution, the gamma evaluation is performed in three dimensions. To facilitate this, a three-dimensional dose distribution is obtained by rescaling the calculated dose for each beam, using ray lines that originate at the source and reach each detector in the arrays. The ratio of absorbed to measured dose at the diode along the ray line is used to calculate the scaling factor [48, 49]. When the comparison is made with another measured dose distribution, the gamma evaluation is limited to the two diode arrays, with linear interpolation used to calculate the dose between the diodes [50].

When used for quality control of RapidArc deliveries, as well as for fixed-beam IMRT, the Delta4 use a trigger pulse from the accelerator to collect the signal from the diodes only during beam-on. The signal for

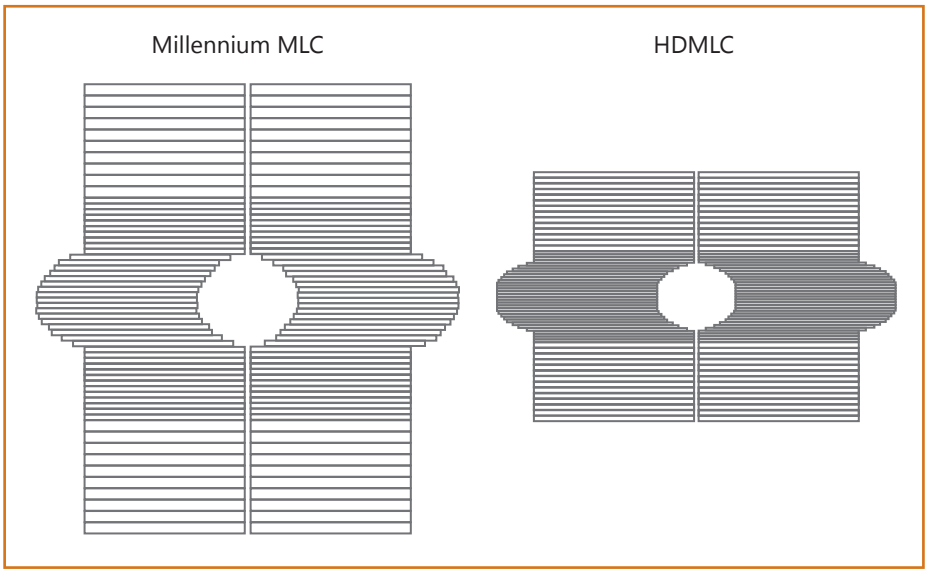

Figure 6. The Millennium 120 MLC and the HDMLC. The heights of the MLCs are represented correctly in the figure, whereas the widths are not (both MLCs have the same width; 37 cm).

each pulse is stored separately and time-dependent evaluation can thereby be done. An inclinometer is attached to the gantry and used by the software to compensate for the directional dependence of the diodes [48]. Owing to the cylindrical shape of phantom and perpendicular diode arrangement, the Delta4 is suitable for quality control of rotationally delivered radiotherapy such as RapidArc [10], Tomotherapy [51] and Elekta VMAT [52].

The Delta4 is the standard phantom for quality control of RapidArc treatments at Rigshospitalet and has previously been used for measurements with MLC-tracking [3, 31]. In the clinical use at Rigshospitalet, the Delta4 is setup at the treatment machine's isocenter according to the laser system in the treatment room, as well as the visual crosshair from the linac treatment head. The phantom is thereafter irradiated with four 15 × 15 cm open fields, 200 MU from four directions (0°, 90°, 180° and 270°), and the measured dose distribution is compared to calculated dose distribution from Eclipse. By comparing the spatial dose distribution this measurement allows for checking and correcting the phantoms position and by comparing the dose deviations a dose correction factor can be obtained. This factor is thereafter applied to the subsequent measurements. This method was used in this study when comparisons were made to the calculated dose, with the difference that only the fields from 0°, 90° and 270° were used to obtains the dose correction factor (since the motion platform affected the results for irradiation at 180°). For evaluation of the measured doses, diodes with doses in the range of 5-500% were used, with 100% being the dose at the isocenter.

2.2.3 Simulating tumour motion

The Standard Imaging Respiratory Gating Platform was used to simulate tumour motion during measurements with the Delta4. The platform allows for sinusoidal motion by means of a rotating disc, with motion amplitudes selectable in discrete steps between 5 mm and 40 mm and with cycle times between 2 and 6 s, with steps of 0.5 s. The experimental setup is shown in Figure 7.

In order to isolate the impact of different plan complexities and different MLCs, the the motion amplitude and cycle time was kept constant for all measurements in this study. A motion amplitude of 2.0 cm and a cycle time of 6 s (peak-to-peak) were chosen to reasonably represent relatively large tumour motion [24].

For the entire study, the center position of the motion platform, i.e. when a cycle would amount to half the motion amplitude in each direction, was used for the setup without target motion. With the motion platform in this position, the Delta4 isocenter was aligned to the isocenter of the linac. When measurements with target motion were performed, the range of motion therefore consisted of motion in the longitudinal direction from -1.0 cm to +1.0 cm, relative to the isocenter. For all measurements with motion the treatment was for consistency started (manually) when the motion platform was at the most cranial position.

For measurements of the latency and geometric accuracy of the MLC-tracking system, a more precise motion platform from Washington University, St Louis, was used. The platform is capable of 3D mo-

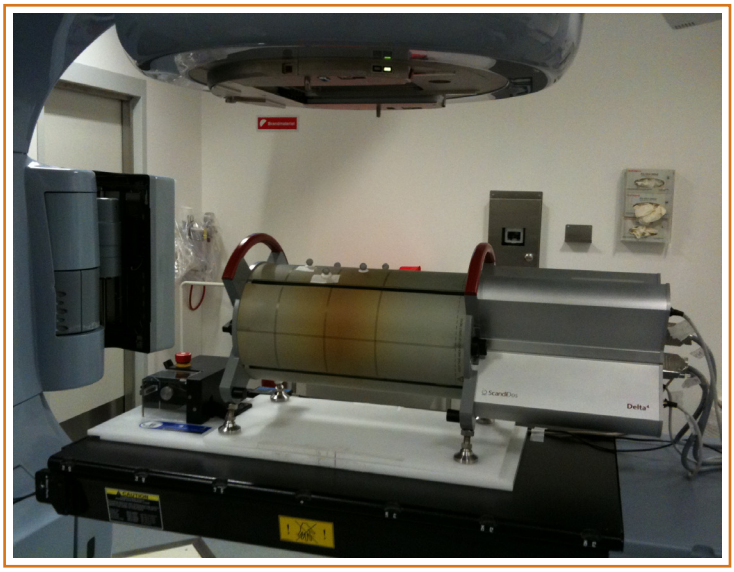

Figure 7. The experimental setup when performing measurements with the Delta4 placed on the Standard Imaging Respiratory Gating Platform. Note the ExacTrac markers placed on the Delta4 phantom.

tion and can be programmed to perform an arbitrary motion pattern within its hardware constraints. This platform was not used for measurements of the treatment plans because of the weight of the Delta4 unit, but was suitable to use for measuring the latency of the MLC-tracking system and its geometric accuracy. The motion platform software reads positional information from a data file with a frequency of 50 Hz.

2.2.4 Monitoring with ExacTrac

During all measurements with MLC-tracking, target monitoring was done with the BrainLAB ExacTrac optical infrared tracking system, which is part of the BrainLAB ExacTrac IGRT suite that also consists of two x-ray sources and detectors. The optical system uses two cameras and reflective markers that are attached to the motion platform, close to the isocenter. When the phantom is correctly located at the isocenter, the marker configuration is saved and the ExacTrac monitoring system thereafter shows the targets displacement relative to the isocenter. Displacements are given for both translation and rotation. Translations are shown in three directions; superior-inferior, left-right and anterior-posterior. Rotational information is given as yaw, roll and tilt, corresponding to rotation along the three translational axes.

The position is updated with a frequency of 20 Hz, and for MLC-tracking purposes the information is transmitted via Ethernet to the MLC-tracking system with the same frequency.

2.2.5 Dosimetric accuracy with MLC-tracking

Gamma evaluation was used to quantify the dosimetric accuracy of the MLC-tracking system and the degradation that is caused by uncompensated motion. This was done in two ways: relative evaluation using measurements as reference, and absolute dosimetry using a calculated dose as reference.

- The measured dose distribution with motion was evaluated against the measured dose distribution without motion (i.e. relative evaluation). This was done both with and without motion compensation using MLC-tracking. For the relative evaluation, measurements with MLC-tracking and moving target were compared to measurements with MLC-tracking and a static target, and measurements without MLC-tracking and a moving target were compared to measurements without MLC-tracking and with a static target. Thus, the effect of the motion was isolated. For these comparisons, gamma criteria of 2% and 2 mm were used to clarify the effect of motion and the performance of the MLC-tracking system.

- The measured dose distribution with and without motion evaluated against the calculated dose distribution (i.e. absolute dosimetry). This was done both for static target (similar to standard quality control) and with moving target both with and without the use of MLC-tracking. When comparing with the calculated dose distribution, gamma criteria of 3% and 3 mm were used, as this is the criteria used for quality control of clinical RapidArc treatments.

For all measurements with MLC-tracking, a prediction algorithm was employed with an assumed latency of 260 ms (based on measurements described in Section 2.3). For patient A, the number of adjacent leafs were set to correspond to 1 cm, i.e. 4 leaves for

delivery with the HDMLC and 2 leaves for the M-MLC. For patient B, for which a tighter jaw setting was used, the numbers of leaves were set to 5 for both MLCs, to resemble the delivery without MLC-tracking where the unused leaves that were not shielded by the jaws were placed at the center of the MLC by the optimization algorithm.

2.3 Measuring the latency and geometric accuracy

As a preparation before performing measurements of RapidArc delivery and MLC-tracking, the latency and geometric accuracy of the MLC-tracking system were investigated. The method used is adapted from Sawant et al. [30]. After measuring the latency using the method described below, the obtained value was used in the motion prediction algorithm.

To measure the latency, the Washington University motion platform described in Section 2.2.3 was used. The same motion pattern was used as for the treatments measurements; i.e. sinusoidal motion with a cycle time of 6 s and a motion amplitude of 2 cm peak-to-peak. The platform was programmed so that the motion revolved around the origin of the platform, which was set up so with the marker was positioned at the isocenter of the linac when the platform was zeroed, using the laser system in the treatment room. With the platform stationary, the isocenter was read into the ExacTrac monitoring software.

At the linac, the motion platform was set up with a metal cylindrical marker was attached to the platform's carrying arm (see photos in Figure 8). The marker had a diameter of 12.0 mm and a height of 23 mm. Mega-voltage imaging was done with the PVI set up for continuous imaging with an imaging frequency of 9.5 frames per second. The MLC-tracking computer was loaded with a circular MLC pattern with a projected diameter of 10 cm at isocenter. The collimator was rotated according to the motion of the platform so that the MLC leaves traveling direction was the same as the marker motion. In this way it was not necessary for additional MLC leaves to open. The jaws were set to 13 cm × 13 cm and the SSD was 100 cm. The MLC-tracking system attempted to place the marker at the center of the BEV at all time.

With a purpose-written MATLAB program, the positions of the geometric centre of the marker as well as the MLC were obtained (Figure 9 and Figure 10). The positions were plotted with respect to time, using the known imaging frequency. With an image with the marker at isocenter, the relative displacement was calculated. The size of the marker was used to determine the number of pixels per millimeter so that the positions could be calculated in millimeters. Sinusoidal functions were fitted to the positions and the displacement, or the phase shift, between the two functions equal to the latency of the MLC-tracking system. Each data set was fitted to the following function:

$$F(t) = A \sin\left[B\left(t + C\right)\right] \tag{5}$$

where C is the phase shift. Using the 'problem solver' in Microsoft Excel, the constants A, B and C were obtained in an iterative process. The latency was then calculated by:

$$\Delta C = C_{marker} - C_{MLC} \tag{6}$$

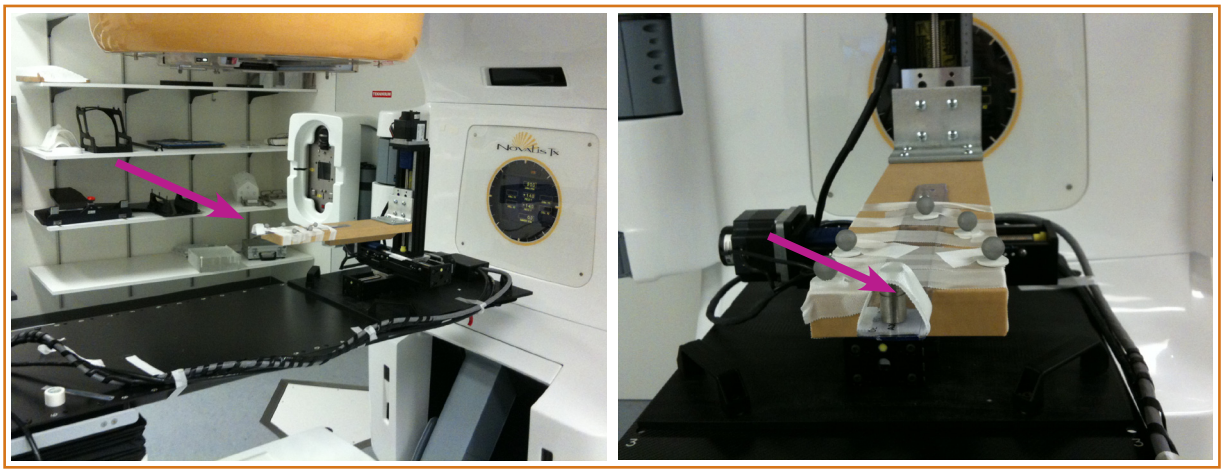

Figure 8. Photo of the experimental setup when measuring the latency and geometric accuracy of the MLC-tracking system, the cylindrical marker is attached to the platforms carrying arm (arrow).

With the latency known, it was used in a motion prediction algorithm, and the experiment described above was repeated. Based on the observation that the prediction algorithm tended to overcompensate for the latency calculated with the equation above, additional measurements were carried out with the assumed latency changed step by step from 200 ms to 260 ms, in steps of 10 ms. The measurement where the chosen assumed latency gave the best agreement was used for evaluating the geometric accuracy of the MLC-tracking system.

2.4 Performance of the ExacTrac monitoring system

This section describes measurements investigating the performance of the ExacTrac monitoring system with regard to accuracy and precision, as well as the effect on RapidArc deliveries. Characterizing the performance of the monitoring system is necessary as any positional error originating there would be interpreted as shortcomings in the MLC-tracking system.

To investigate the performance of the ExacTrac monitoring system with regards to its ability to correctly report the position of a phantom placed on the treatment couch, comparisons were made between the re-

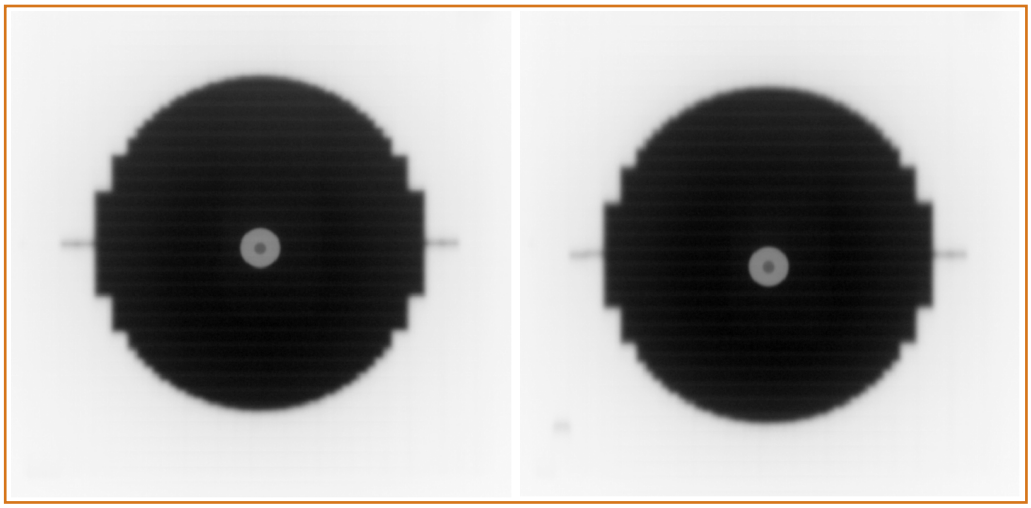

Figure 9. PVI images showing the marker at or near the center and the MLC shape. In the left image, the marker is stationary and in the right image the marker is moving and no prediction is used.

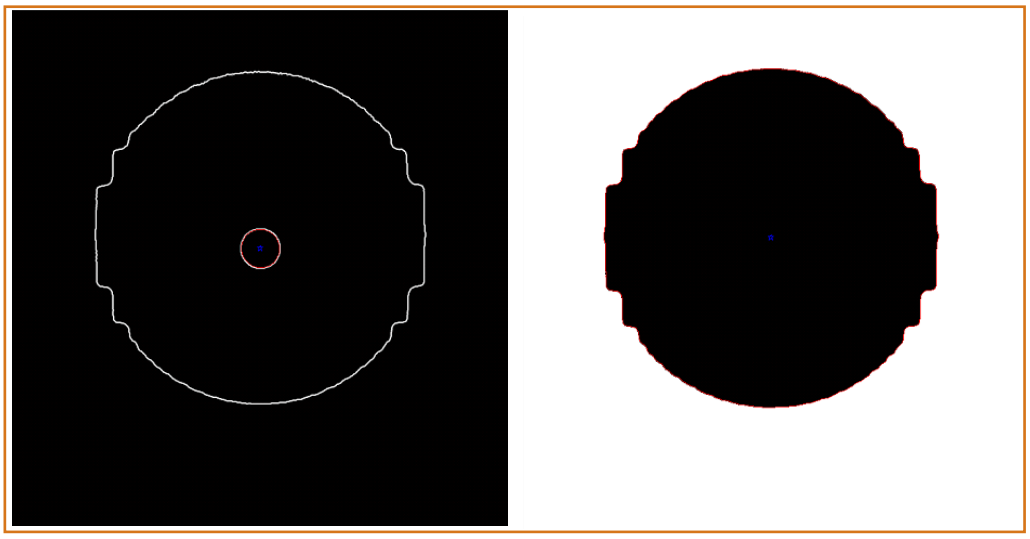

Figure 10. Screenshots from MATLAB segmentation of the marker (left) and MLC shape (right). The centers of the acquired areas were used in the evaluation.

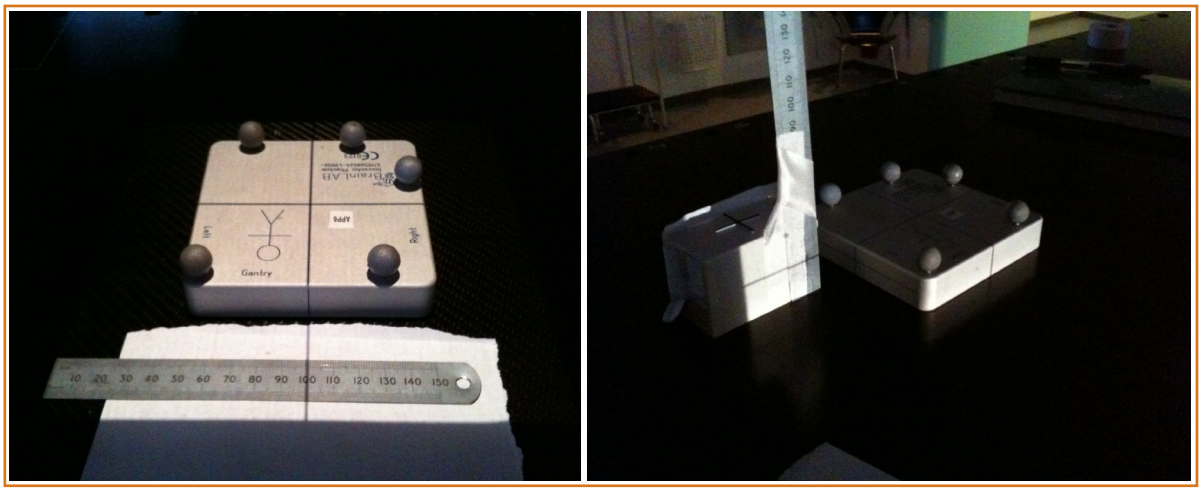

Figure 11. Experimental setup for measurements with ExacTrac with a steel ruler as reference in the superior-inferior and left-right direction (left) and anterior-posterior direction (right, gantry rotated to 270°). Notice the crosshair from the treatment head that is used to determine the true position.

ported position from ExacTrac and the true position measured with a steel ruler. The couch was moved in the anterior-posterior, left-right and superior-inferior directions on at a time, with displacements of +2.0 cm (+1.9 cm in the AP direction), +1.0 cm, 0.0 cm, -1.0 cm and -2.0 cm relative to the isocenter. The reported position was recorded with a frequency of 20 Hz. Each displacement was done three times, and each direction considered as a single measurement. The deviation from the ExacTrac position compared to the ruler, i.e. the positional error, was calculated for each measurement, with data collected during the movement of the couch removed. The mean error, the standard deviation of the error and the root-mean-squared of the error[1] were calculated.

To quantify the effect of noise as well as to determine if there was any positional drift in the ExacTrac system, the reported position was measured for a static target during approximately 30 min. The position was recorded with a frequency of 5 Hz and the mean, standard deviation and root mean squared were calculated.

2.4.1 Investigation of the degradation of the delivery caused by using the monitoring system

In order to determine the influence of noise in the ExacTrac monitoring system on RapidArc delivery with MLC-tracking, the MLC-tracking system was connected and the target kept static. Four RapidArc plans were delivered using input from the ExacTrac monitoring system. A data file with positional information for a static target then used as input, and the measurements were repeated, thus allowing for a comparison with the effect of noice and drift in the ExacTrac monitoring system isolated. The measured dose with a data file as input was used as reference in the Delta4 evaluation software. No prediction algorithm was used in these measurements.

2.5 Statistical analysis

Statistical analysis was used in two cases in this study. The first in to determine if there is a significant differnce between the two MLCs with regards to the geometric accuracy with MLC-tracking. The accuracy for each assumed latency for one MLC is considered a measurement, and paired with the the accuracy for the other MLC. The two-tailed paired t-test therefore used. Secondly, statistical analysis is used to determine if there is a significant difference in MLC-tracking performance when using the two different MLCs. As the plans were created with the same planning objectives and constraints for the two MLCs, the result for one MLC can be compared with the result for the plan created with the same objectives for the other MLC. The two-tailed, paired t-test is used also in this case. This comparision is done for both relative evaluation and absolute evaluation (i.e. absolute dosimetry).

1 RMS = $(\text{mean}^2 + \text{standard deviation}^2)^{-1/2}$

3 Results and discussion

In this section, the geometric accuracy with MLC-tracking measured using EPID-imaging and the dosimetric accuracy quantified with the gamma evaluation method are first presented. Thereafter the ability of the adjacent leaf distance and number of monitor units to predict the MLC-tracking performance are shown. The issue of central overdosage as well as dose profiles follows, and finally results showing the performance of the ExacTrac monitoring system are presented. For each part a discussion follows directly after the results.

3.1 Geometric accuracy

See Figure 12 and Table 6 (appendix) for the geometrical accuracy expressed as the root-mean-square error (RMS) in millimeter for the HDMLC and the M-MLC, for different assumed latencies and for a motion pattern of 2 cm peak-to-peak amplitude and 6 s cycle time. For the measured MLC and marker positions for the two MLCs, as well as the geometric error both with and without prediction, see Figure 13. A two-tailed paired *t*-test comparing the RMS error for the two MLCs did not show a significant difference, even though the P-value was quite low (P = 0.09).

The geometric accuracy, expressed as the error root mean squared, was thus found to be better than 0.5 mm for both MLCs and for all the investigated choices of prediction parameters. With the optimal prediction setting, a geometric accuracy of 0.32 mm (HDMLC) and 0.35 mm (M-MLC) was achieved. With a motion amplitude of 2.0 cm peak-to-peak, MLC-tracking seemed to be very capable of compensating for the motion. The geometric error seemed to be the largest at the end points of the motion, suggesting that the error might be further reduced with improvements in the prediction algorithm.

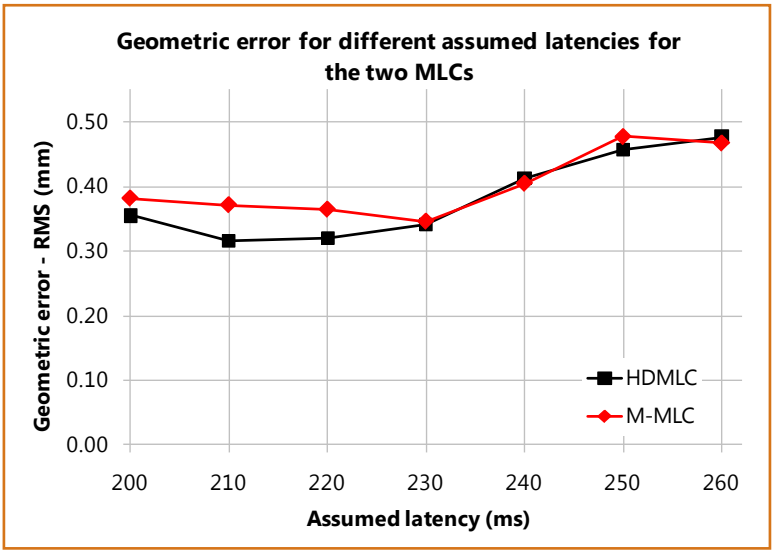

Figure 12. The geometrical error for different assumed latencies for the two MLCs.

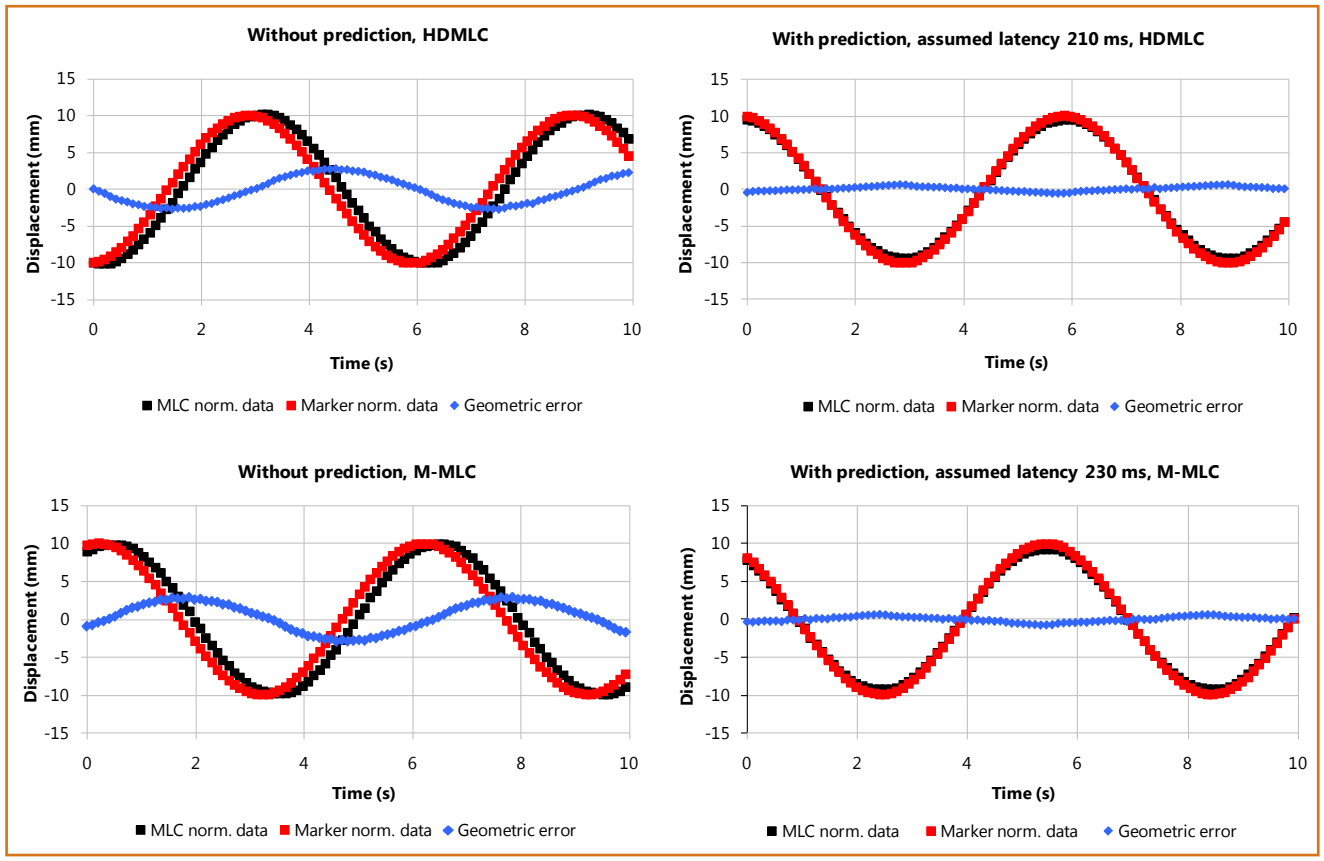

Figure 13. The measured positions of the marker and MLC centers, as well as the geometric error for the HDMLC (top) and the Millennium MLC (bottom), without using a prediction algorithm (left) and using prediction with an assumed latency of 210 ms and 230 ms respectively (right).

The difference in geometric accuracy for the two MLCs was small and not significant (P = 0.09). The low p-value does however hint that there may be a difference, favoring the HDMLC. The unexpected decrease for the Millennium MLC when the assumed latency was increased from 250 ms to 260 ms suggests that the uncertainty in the results is at least 0.01 mm. Further studies of motion perpendicular to the MLC leaves as well as irregular motion patterns might be of interest to further characterize the geometric capabilities and limitations of MLC-tracking. The results confirm that MLC-tracking using the BrainLAB monitoring system allows for sub-millimeter geometric accuracy [30, 37].

3.2 Dosimetric accuracy

Measurements of RapidArc deliveries with MLC-tracking were performed with the Delta4 dosimetric device allowing the gamma index evaluation to be used for comparison. In total, measurements were performed on 44 different treatment plans. Different combinations of MLCs, collimator angles and different parameters in the treatment planning were investigated.

3.2.1 Relative evaluation

See Figure 14 for the results of measurement with and without tracking for a moving target, using measurements with a static target as reference. A few trends can be seen: the pass rate is higher with MLC-tracking than without, a few plans, namely the ones with a leaf distance constraint and the a few of the simplest plans from the clinical TPS, showed an high pass rate of over 97 %. More strigent planning criteria were hinted to mean a decreased the pass rate, especially for the first patient. With a collimator angle of 88°, all plans showed a high pass rate with MLC-tracking, regardless of the plan complexity.

The results of relative measurements used gamma criteria of 2% and 2 mm which allowed for the differences to be clearly distinguished. By using measurements with a static target as reference, the effect of the motion and the capability of the MLC-tracking system to compensate was isolated from other factors such as errors in dose calculation and set up. This also allowed using such stringent criteria as 2% and 2 mm.

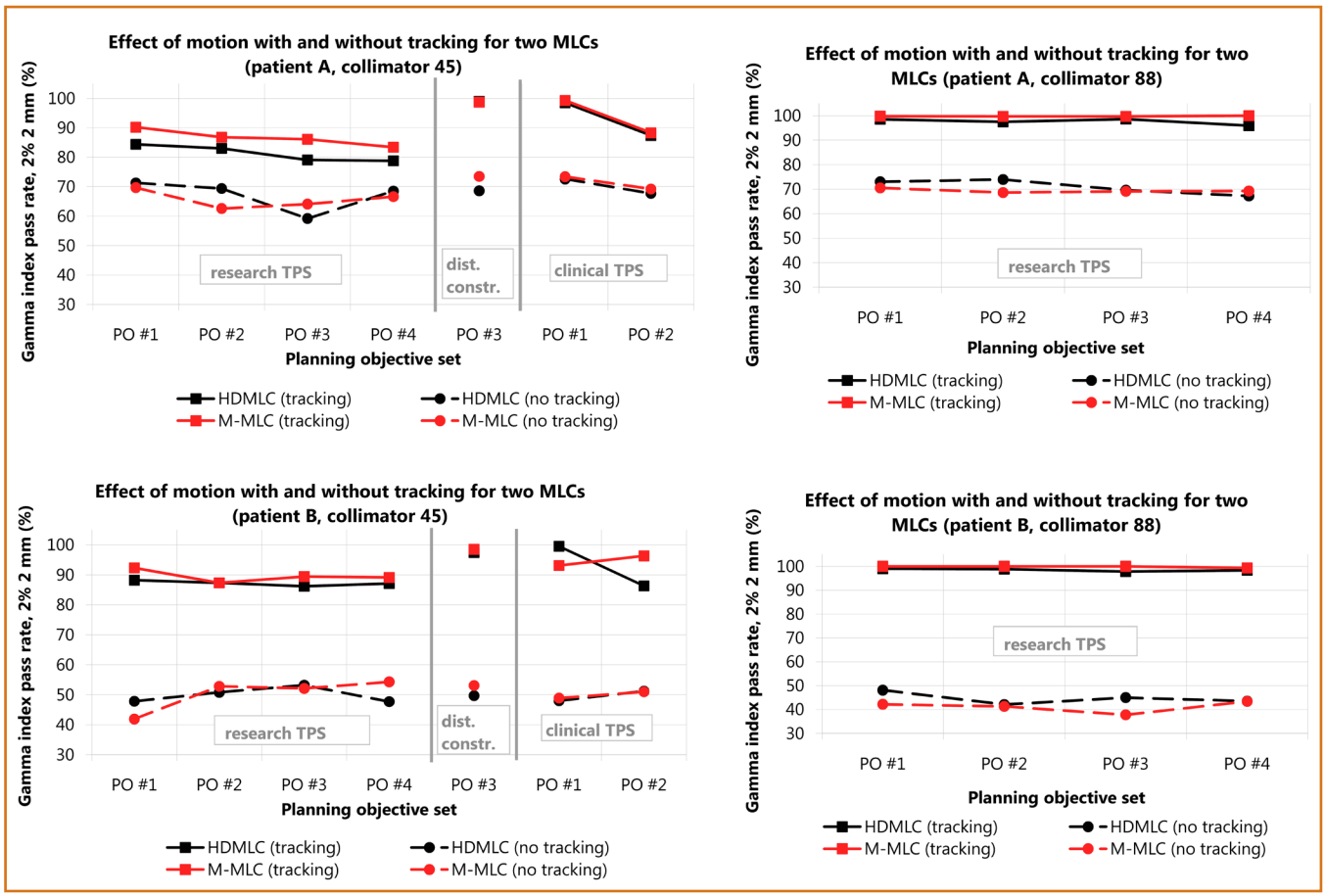

Figure 14. Results of relative measurements for the two patients with and without MLC-tracking for deliveries to a moving target, using measurements with a static target as reference.

The results showed that MLC-tracking greatly improved results compared to not using motion compensation for all plans. An absence of motion compensation resulted in dose blurring (see Section 3.2.5) and possibly also interplay effects which might show as single diodes showing relatively higher or lower dose, compared to adjacent diodes. However, the interplay effect cannot with certainty be distinguished from dose blurring by using this method. For patient B, where the PTV size in the superior-inferior direction was 2.6 cm, the motion caused gamma evaluation failures to a larger extend than for patient A where the size was 5.3 cm.

The use of a collimator angle of 88° gave superior MLC-tracking performance compared to a collimator of 45° for all but a few of the investigated plans. For these plans however, the gamma index pass rate with MLC-tracking and moving target approached 100% (for the four plans with the best results: 99.5%, 97.4% 99.0% and 98.5% (HDMLC), 99.3%, 98.7%, 96.3% and 98.5% (M-MLC)). These plans were the plans created in the clinical TPS with the most relaxed objectives (PO #1, except for patient B and the M-MLC where PO#2 gave better results), and the plans with constraints on the distance to adjacent MLC leaves. For all plans with a collimator angle of 88°, the pass rates were larger than 95%, and larger than 97% for all plans but one.

Statistical analysis with the two-tailed paired *t*-test showed that MLC-tracking with the Millennium MLC gave significantly better tracking results than using the HDMLC (P=0.003). That the pass rate was significantly higher for the M-MLC compared to the HDMLC might be caused by the fact that fewer leaves were used to compensate for the motion; for a target displacement of one centimeter, at most two leaves would be shifted with the M-MLC compared to four on the HDMLC. With fewer leaves shifted, the risk of an adjacent leaf of being too far away for effective compensation is decreased. It is also likely that the higher resolution allowed for the plans to have complicated shapes as the optimizer had about two times as many leaves to use for modulation of the plans. The fact that the plans created with the most relaxed objectives, i.e. the least modulated plans, showed similar MLC-tracking performance

for the two MLCs supports this argument. The performances for plans with a constraint on the adjacent leaf distance were very similar indicating that there is no intrinsic disadvantage with using the HDMLC for MLC-tracking.

A difference in MLC-tracking performance for plans with the same planning objective set but created in different versions of Eclipse was clearly seen from the results. For PO#1, the simplest planning objectives, all plans created in the clinical version of Eclipse had better MLC-tracking performance than corresponding plans created in the research version. To divulge into differences in optimization and dose calculation algorithms for the two versions is beyond the scope of this study, and any difference is complexity would need to be investigated for a larger number of cases. That said, it seemed that the clinical version was capable of creating simpler plans with regard to the average adjacent leaf distance, therefore increasing the MLC-tracking performance. It should be stressed that the planning objectives for PO#1 was clinically unrealistic in the sense that the optimization algorithm did not have to compromise between target coverage and sparing of risk organs, as the objectives for the risk organs were (intentionally) set very loose.

Previous studies that investigated the accuracy of MLC-tracking of RapidArc treatments with the Delta4 differed from this study in two major aspects; the monitoring system used was characterized by larger uncertainties and no prediction algorithm was used [3, 31]. By using a prediction algorithm and a highly precise monitoring system, measurements in this study were carried out with excellent accuracy. The results obtained in previous studies showed no significance difference in using collimator angles of 45° and 90°, in stark contrast with the results shown here. This disparity is explained by two factors; the difference in methodology mentioned above, and the difference in plan complexity. The study by Falk et al. [3] investigated RapidArc-plans that based on the number of monitoring units were of a complexity that somewhat corresponds to the simpler plan created in the clinical TPS and for the Millennium MLC. For this plan, the MLC-tracking performance with a 45° collimator angle was excellent. The results obtained here are therefore not in conflict with the referred studies but instead to be considered as an addition to them.

The results showed conclusively that the motion component that was perpendicular to the MLC leaves was the cause of gamma evaluation failures and that this depends on the specific treatment plan, and confirms that it is possible to geometrically compensate for target motion with MLC-tracking.

3.2.2 Absolute dosimetry with MLC-tracking

In Figure 15 and Figure 16 the results of measurements with moving target, with and without MLC-tracking, as well as with a static target (without using MLC-tracking) are shown. The calculated dose is used as the reference dose.

Comparisons of deliveries with MLC-tracking with calculated dose distributions are associated with certain problems that affect the results. Among these are the fact that unused MLC leaves were moved to the side by the MLC-tracking system, that MLC-leaves that were kept ready constantly were moved adjacent to the nearest open pair, as well as off-axis effects.

Leaves that were moved to the side caused underdosage when compared to the calculated dose, as the leaves that were placed in a closed state at the center of the MLC in the treatment planning system caused leakage irradiation. As the jaws were set wider for patient A than for patient B, leaves were moved to the side only for patient A. The impact of this can be seen in the comparison with the calculated doses for the two patients. The continuous movement of adjacent leaves resulted in the dose from interleaf leakage being blurred and therefore not in agreement with the planned dose. Lastly, the radiation beam was not entirely uniform for an open field, as the beam was filtered to obtain a uniform beam at the depth of 10 cm, and moving the MLC (and therefore the beam) about a centimeter was excepted to have some, albeit likely negligible, effect.

These effects lead to the conclusion that caution should be taken when comparing the measured and the calculated dose distributions, however, some conclusions can still be drawn.

For patient A, as described in Section 2.2.5, the jaws were set to 13 cm × 13 cm, even though the target was considerably smaller. This meant that a number of leaf pairs were unused (as seen in Figure 1). The difference when using MLC-tracking was therefore that approximately 6 leaf pairs were moved to the side. For patient B, on the other hand, the jaws were set closer which meant that no leaves were moved to the side. This was likely the explanation for the worse results seen in Figure 15 compared to Figure 14, for example for the plan with collimator angle 45° that had an adjacent leaf distance constraint ("CA 45, dist. constraint"). For patient A, the pass

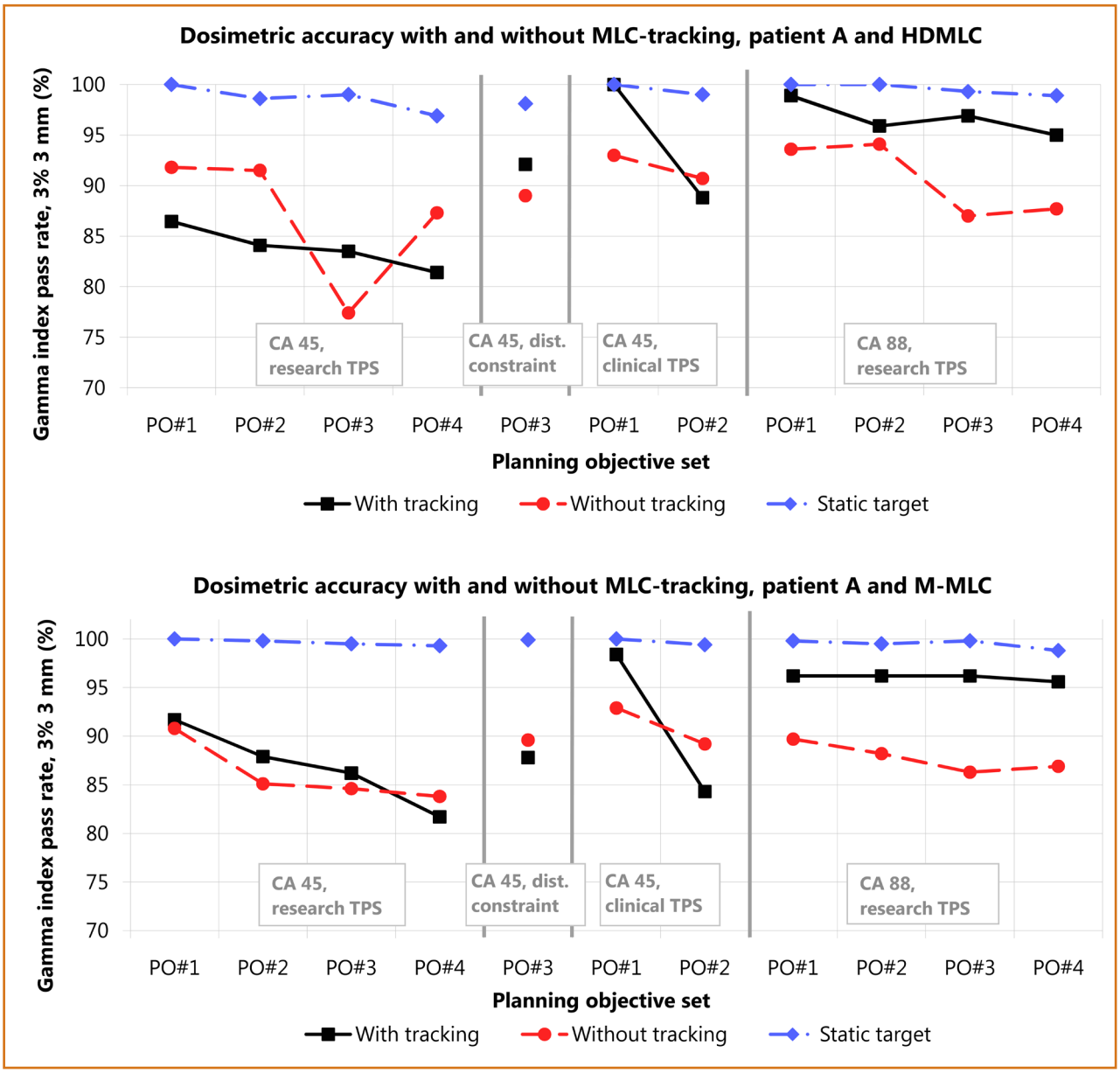

Figure 15. Results of measurements for patient A and the two MLCs with and without MLC-tracking (moving target), and without MLC-tracking (static target), the calculated dose used as reference.

rates for those plans when compared to the calculated dose were around 90% in contrast to about 99% for the relative measurement (which also used more stringent gamma evaluation criteria). For patient B, the corresponding plans gave results around 95% for comparison with the calculated dose, supporting the argument that the jaw setting was the cause of the difference.

For a few plans, the pass rate was higher than 99%. These included all plans with a collimator angle of 88° for patient B and the Millennium MLC, and the plans created with the clinical version of Eclipse and PO#1 for both patients for the HDMLC. These plans had in common that the static measurement gave pass rates higher than 99.8 %. This shows that it was possible to obtain very good agreement with measurements with MLC-tracking compared to calculated dose, despite the problems associated with such a comparison. However, the fact that some plans that gave very high pass rates (>99%) for relative measurements obtained pass rates as low as 88% when compared to the measured dose shows the need for further investigation if this is a method that should be used for MLC-tracking measurements. It would be of interest to create plans with a distance constraint as well as a monitor unit objective of for example 600 MU, as the plans tended to have a large number of monitor units and some control points with only a few open MLC leaves, a difficult scenario

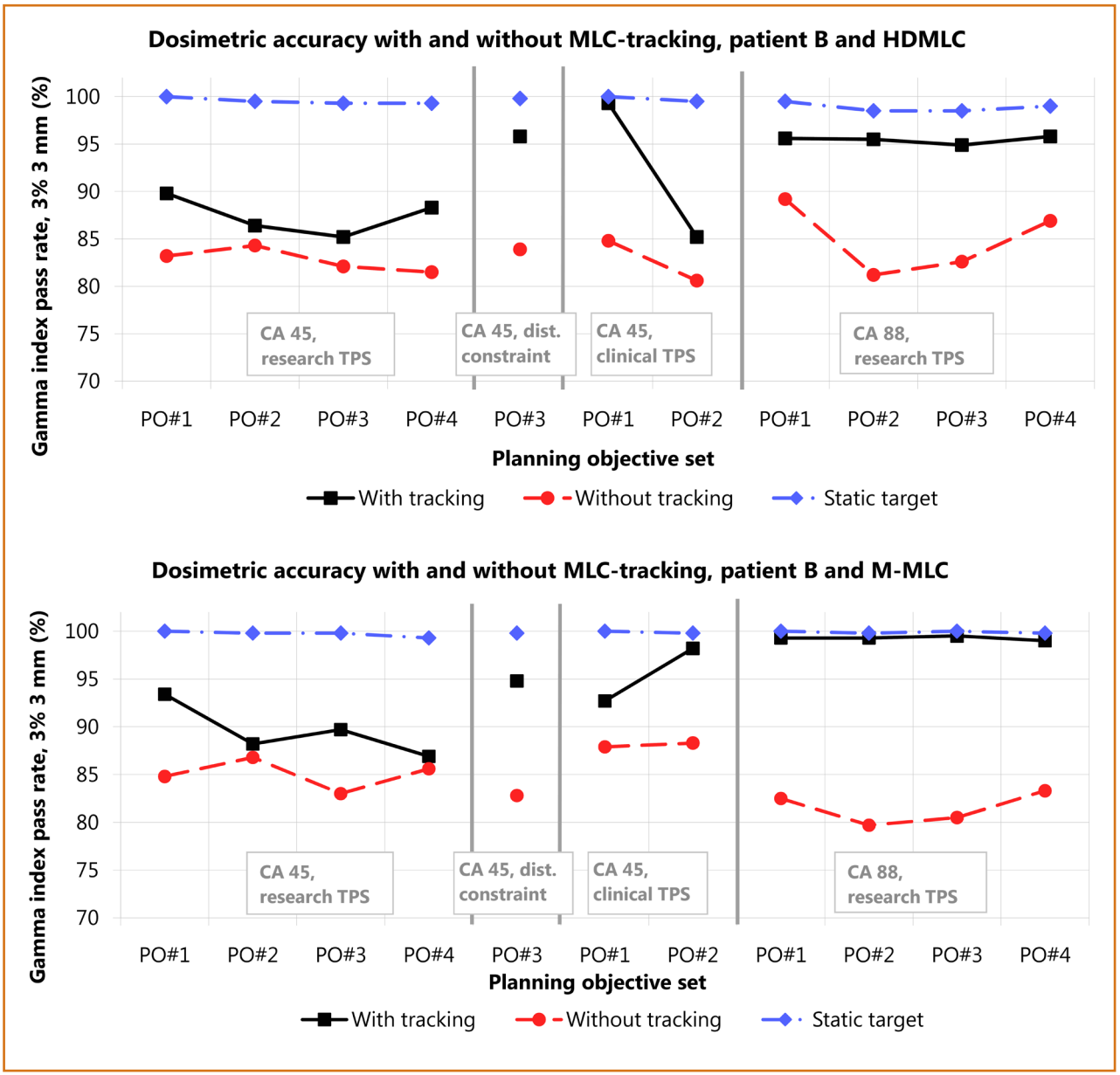

Figure 16. Results of measurements for patient B and the two MLCs with and without MLC-tracking (moving target), and without MLC-tracking (static target), the calculated dose used as reference.

with regards to accurate dose calculation (Section 1.2.4).

Statistical analysis with the two-tailed paired t-test showed no significant difference between the two MLCs (P=0.167) when the calculated dose was used as reference. This result was in contrast to the result in the previous section when measurements were used as reference. The problems associated with comparisons with the calculated dose are likely to explain the difference.

As the gamma index pass rate that was required for a treatment plan to be clinically accepted was 95% at Rigshospitalet (along with other criteria such as the amount of overdosage), several plans with MLC-tracking would, based only on the gamma index pass rate, be clinically accepted for treatment. In contrast, no treatment of a moving target without the use of motion compensation achieves a pass rate of 95%.

3.2.3 MLC-tracking performance with regards to adjacent leaf distance

Figure 17 shows the gamma evaluation pass rate (2% 2 mm) for plans with collimator angle 45°, plotted against the weighted average leaf distance calculated for all but the most peripheral leaves (also see Section 2.1.3). The results showed a clear correlation between increased adjacent leaf distance and decreased

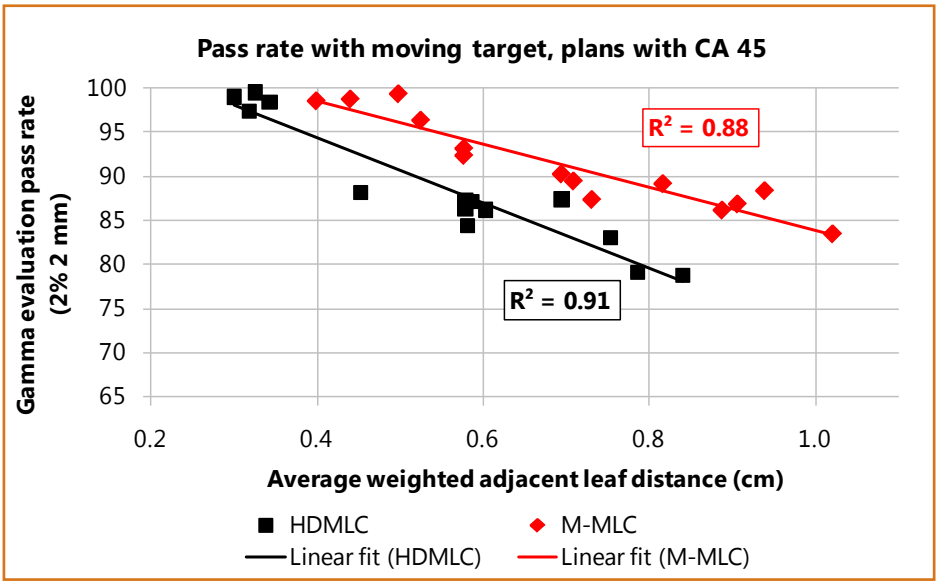

Figure 17. The pass rate with MLC-tracking and moving target, using measurement with a static target as reference, for all plans with collimator angle 45°, plotted with respect to the weighted average adjacent leaf distance.

pass rate, with a linear fit giving $R^2 \approx 0.9$. As there was no reason to assume that any relationship would be linear this should be interpreted only that there was a relationship without characterizing it as such. A logarithmic fit, for example, gave a slightly better fit with $R^2 = 0.93$ (HDMLC) and $R^2 = 0.91$ (M-MLC).

The observed correlation supports the conclusion drawn in Section 3.2.1 that it was motion perpendicular to the MLC leaves that for some plans caused gamma evaluation failures. When the distance to adjacent leaves was small, the MLC-tracking system was very well capable of motion compensation, whereas when the distance became too large, under- or overdosage occured leading to gamma evaluation failures.

As it was noted that the utmost leaves were moved aside and placed near the jaws for some treatment plans, these leaves were not included in the calculation. The leaves were regarded by the MLC-tracking system as part of the MLC and hence adjusted for target motion. The adjacent leaves were therefore placed next to the moved leaf pair, far from the center, something that might have decreased the MLC-tracking performance. The rationale for still not including these leaves in the calculation is threefold; (1) the leaves that were moved to the side strongly influenced the average distance, (2) the treatment plans that gave bad results with MLC-tracking and a moving target showed dose deviations in the high dose region near the isocenter, whereas the dose distribution at the edge of the target was well maintained (this suggests that the effect of leaves being moved to the side was minimal) and (3), it allowed for comparison of all treatment plans without regards to whether the plan contained leaves that were moved to the side.

The observed correlation suggests that the adjacent leaf distance is a parameter of great interest for determining if a treatment plan is suitable for MLC-tracking. For a clinical implementation, these results suggest that using a constraint on the adjacent leaf distance in the treatment optimization would be a suitable approach when creating treatment plans. Further work could possible determine the maximum allowed distance that still gives satisfactory MLC-tracking performance.

3.2.4 MLC-tracking performance with regards to number of monitor units

Figure 18 shows the pass rate (for 2% and 2 mm) for plans with collimator angle 45° as a function of the number of monitor units used in the plan, using static measurements as reference. As the plans optimized with a constraint on the distance to adjacent leaves were expected to increase the MLC-tracking performance without respect to the number of monitor units, these are not included in the comparison (the number of monitor units for these plans were high and yet showed excellent MLC-tracking results).

The weak correlation observed between gamma index pass rate and numbers of monitor units used in the treatment suggest that the number of monitor

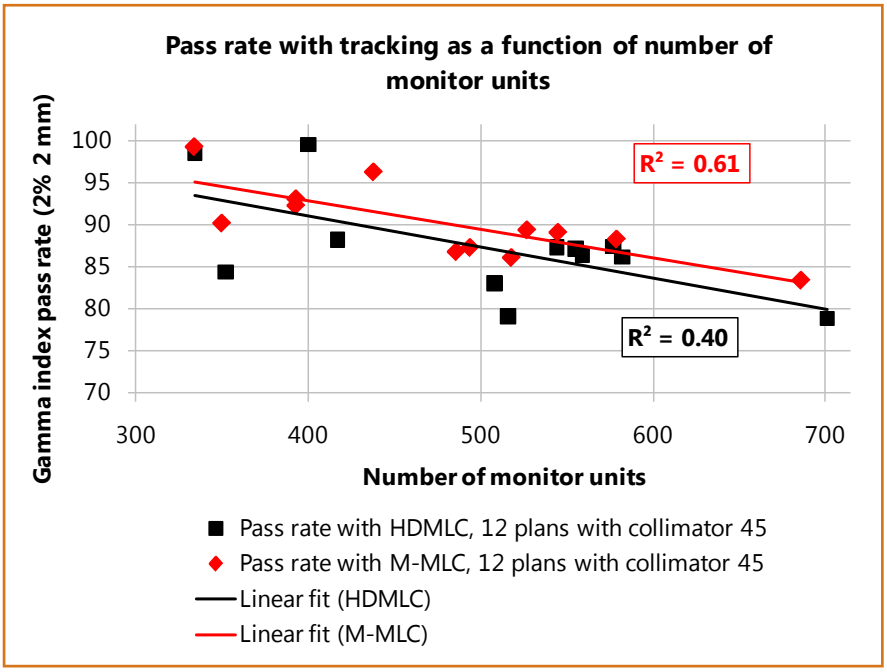

Figure 18. The pass rate with MLC-tracking and moving target, using measurement with a static target as reference, for all plans with collimator angle 45°, plotted with respect to the number of monitor units used in respective plan.

units is not a suitable parameter for describing the performance of MLC-tracking. For the measurements without MLC-tracking and without motion (the blue dodded line in Figure 15 and Figure 16), a slight tendency was noted with decreased pass rate with more stringent planning criteria. This occured especially for patient A and with the HDMLC. This might suggest that the number of monitor usnits may still have some use as a parameter to describe plan complexity per se, just not in the context of MLC-tracking.

3.2.5 Dose profiles

Figure 19 shows dose profiles for the central diodes in the superior-inferior direction, for two plans showing examples of both excellent motion compensation and central overdosage. The two dose profiles were representative for the case of MLC-tracking success (left) and failure (right). The pass rate with relative measurements was 99.5% (left) and 86.2% (right).

It could be seen in the right plan that the MLC-tracking system is able to compensate for the motion in the sense that the dose gradients are very similar to the static measurement. The problem was instead overdosage in the central area. The amount of overdosage was plan dependant and generally higher for the HDMLC compared to the Millennium MLC. Plans with a high pass rate had, unsurprisingly, less overdosage as only one plan with a pass rate higher than 95% had any diodes with more than 5% overdosage.

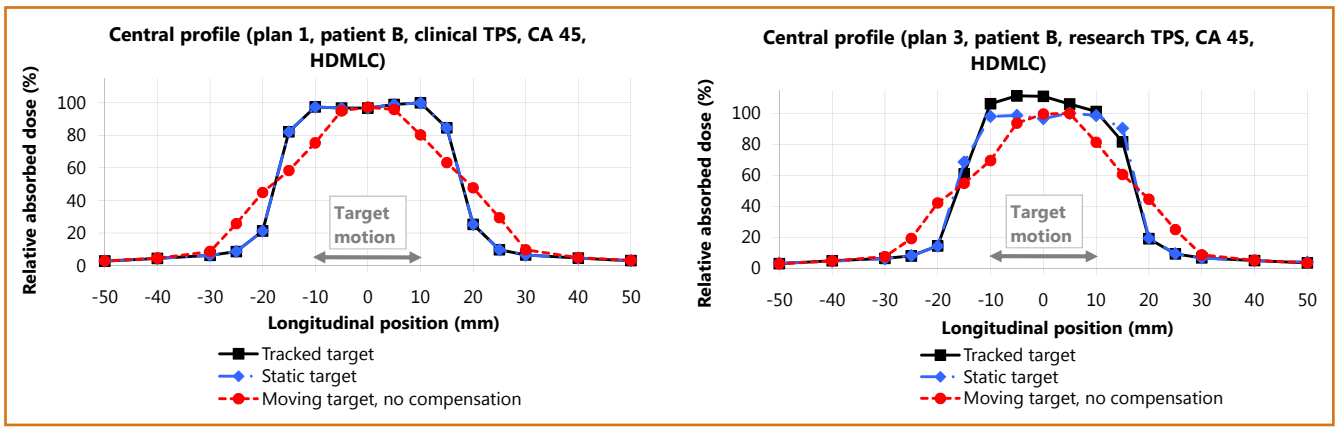

Figure 19. Two central dose profiles in the superior-inferior direction, showing examples of when MLC-tracking gives very good motion compensation (left, pass rate 2% 2 mm: 99.5%) and causes central overdosage (right, pass rate 2% 2 mm: 86.2%).

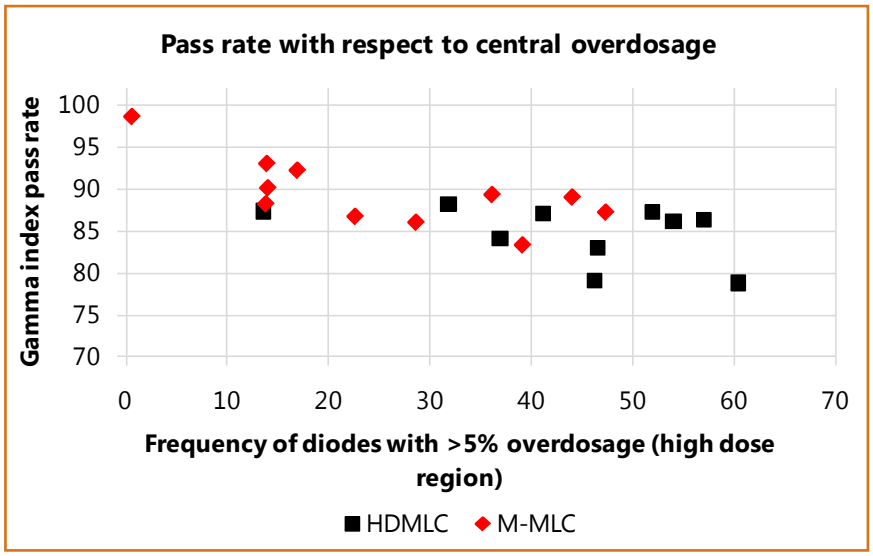

Figure 20. Pass rate with MLC-tracking and a moving target for the two MLCs, plotted against the frequency of diodes in the high dose region (90-500%) with >5% overdosage. Measurement with a static target was used as reference in the gamma evaluation.

3.2.6 Central overdosage

For the treatment plans that gave poor results with MLC-tracking (i.e. with gamma index pass rates < 90% using relative measurements and 2% 2 mm criteria), analyses of the dose profiles implied that the main issue was overdosage in the high dose regions. An example is seen in Figure 19 (right). The dose gradients were generally well maintained. Therefore, the frequency of overdosage (defined as >5% overdosage for diodes in the dose region of 90-500%) was extracted from the measurements. No plan with a collimator angle of 88 degrees showed this overdosage. A weak tendency for decreased pass rate was seen for increased overdosage frequency, and the amount of overdosage was generally higher for plan delivered on the HDMLC compared to the M-MLC.

3.3 Uncertainty of the results

As the combinations of planning objective sets, patient and type of MLC created a large number of different plans, only a few measurements were repeated to investigate the uncertainty of the gamma evaluation results of deliveries with MLC-tracking. These are summarized in Table 4. Even though the numbers of measurements investigating the repeatability were few, the small deviation in the results suggests that the conclusions drawn in this study are valid.

Table 4. Results of repeated measurements for a few plans with MLC-tracking of a moving target, using a static measurement as reference and gamma criteria 2% 2mm.

Plan properties (collimator angle and MLC)	Mean value (%)	Max / min or standard deviation (%)	Number of measurements
CA 45, HDMLC, plan A09-HDMLC	98.5	98.4 / 98.6	2
CA 45, HDMLC, plan A10-HDMLC	87.4	87.1 / 87.7	2
CA 45, HDMLC, plan A01-HDMLC	84.1	83.8 / 84.4	2
CA 88, HDMLC, plan A05-HDMLC	98.5	0.26	5
CA 88, HDMLC, plan A06-HDMLC	97.5	0.04	5
CA 88, HDMLC, plan A07-HDMLc	98.5	0.09	5
CA 88, HDMLC, plan A08-HDMLC	95.9	0.24	5
CA 88, M-MLC, plan A08-M-MLC	100.0	0.09	5

Table 5. Positional error measured with the ExacTrac monitoring system, steel ruler used as reference. For each translation, the couch was moved 18 times with +2 cm, +1 cm, 0 cm, -1 cm and -2 cm displacement and the error relative to the ruler was used for evaluation.

Translation	Mean position error (mm)	Standard deviation of position error (mm)	RMS of position error (mm)	Number of data points
Anterior-posterior	0.00	0.128	0.128	2797
Left-right	0.04	0.054	0.070	2792
Superior-inferior	-0.06	0.079	0.101	2791
Noise (static target at isocenter)	0.03	0.023	0.038	8760

3.4 Performance of the ExacTrac monitoring system

Shown in Table 5 are the results of measurements in the anterior-posterior, left-right and superior-inferior directions where the couch was moved three times to +2.0 cm (+1.9 cm for in the anterior-posterior direction), +1.0 cm, -1.0 cm and -2.0 cm, with a steel ruler used as reference. When calculating the error, data collected when the couch was moved were removed.

Figure 21 (appendix) shows the measured position and the position error for the three directions, as well as unfiltered data for displacements in the superior-inferior direction. Figure 22 (appendix) shows the error in the measured position (calculated by normalizing to the mean) reported by ExacTrac for a static target during approximately 30 minutes of measurement. The pass rate for measurements with static target and input from the ExacTrac monitoring system, when using measurements with a data file containing static information is shown for four plans in Figure 23 (appendix).

The measurements showed that the accuracy of the monitoring system was excellent, especially when considering the accuracy of the reference measurement with the ruler. A slight offset in the adjustment of the couch could likely cause the errors that were observed. No positional drift was observed during approximately 30 minutes of measurement. Comparison of the delivery with a static target and a data file showed that the influence from the ExacTrac monitoring system was minimal and that it was not a cause for any considerable degradation of the delivery. The fact that the geometric accuracy was excellent (Section 3.1) was also a confirmation that the monitoring system worked well.

3.5 The latency of the MLC-tracking system

Using the method of fitting sine functions to the obtained MLC and marker positions, described in Section 2.3, the phase difference was calculated to be approximately 260 ms for both the HDMLC and the M-MLC. When performing measurements of the geometric accuracy, the assumed latencies that gave the highest accuracy were 210 ms for the HDMLC and 230 ms for the M-MLC.

The cause of the difference is not clear. Two subsequently measurements of the latency gave results that differed with 23 ms for the M-MLC (241 ms and 264 ms) hinting that the uncertainty in the measurements might be considerable. The method of changing the assumed latency stepwise was on the other hand a more direct method of measuring the latency and seems to be less sensitive to errors.

As the assumed latency that was used for all measurements was 260 ms, a small improvement in the gamma evaluation pass rate could be expected with the correct assumed latency. One plan was measured with the assumed latency of 210 ms on the M-MLC (which at the time was assumed to be the true value), giving an increased gamma index pass rate of 0.3 percent points; from 92.7% to 93.0% (3% 3 mm, comparison with calculated dose). Thus, the pass rate was likely to only increase slightly with the correct prediction parameter and the results obtained using 260 ms are valid.

4 Conclusions and future prospects

The results obtained in this study shows that it was possible to use MLC-tracking during RapidArc delivery to compensate for the simulated target motion. The geometric accuracy of the MLC-tracking system has also been investigated with satisfying results. Compared to not using motion compensation, the gamma index pass rate was increased using MLC-tracking, even though the performance tended to decrease for more complex plans. A clear correlation was observed between increased average adjacent leaf distance (weighted against the dose weight for the corresponding control point) and decreased gamma index pass rate. This indicates that the adjacent leaf distance was the key factor for MLC-tracking to perform well with RapidArc. The plans with the smallest adjacent leaf distance was also the plans that gave the best results, and for these plans the MLC-tracking system was able to completely compensate for the target motion. Further work looking into the use of a constraint on the adjacent leaf distance is underway at Rigshospitalet.

Aligning the leaves with the target motion substantially increased the gamma index pass rate for both MLCs, regardless of the plan complexity. It would therefore be of interest to evaluate the performance of MLC-tracking with realistic target motion patterns that also include motion in the left-right and anterior-posterior directions for plans with a collimator angle of 88°. A treatment planning study that compares plans with a collimator angle of 45° with the adjacent leaf distance constraint with plan using an 88° collimator angle would be motivated, should these measurements show that the 88° collimator angle is useful also for realistic target motions.

The pass rate was significantly higher for measurements using the Millennium MLC compared to the HDMLC. This was likely caused by the fact that fewer MLC leaves were needed to compensate for the motion with the Millennium MLC and that the more complicated MLC-shapes were possibly with the HDMLC. The similar tracking performance for the least complicated plans (such as the plans with a constraint on the adjacent leaf distance) supports this conclusion.

With collimator angle 45° some overdosage occurred for plans that also tended to show a large extend of gamma evaluation failures. Analyses of the dose profiles indicated that this was the main cause of the decreased pass rate, as the dose gradients were generally well maintained with MLC-tracking. Calculation of the adjacent leaf distance indicates that the problem was that some leaves needed to travel too far to compensate for the motion, leading to dosimetric errors.

As this technique of motion compensation was preclinical, there are several developments that are needed to be done before any clinical use is possible. These include creating methods of quality assurance and development of methods to accurately calculate the dose distribution with MLC-tracking. To develop tools to determine how suitable a treatment plan is for MLC-tracking, possibly including the use of the distance to adjacent leaves or simulating a treatment, would be useful to exclude plans that are not expected to work well with MLC-tracking.

It would also be of interest to look into the use of MLC-tracking for stereotactic body radiotherapy of the lung. These treatments are characterized by the dose per fraction being considerably higher which is expected to result in less interplay effects and increased dose averaging when not using motion compensation. The potential of MLC-tracking for these treatments therefore needs to be determined.

To only use external markers is not satisfactory for a clinical implementation of MLC-tracking, as the

external motion needs to be correlated to the internal target motion. This can be done by the use of imaging or implanted transponders. In order to limit the amount of irradiation caused by the monitoring system, monitoring with external markers could possibly be complemented by imaging. The use of megavoltage imaging with the treatment beam would lead to no extra dose to the patient. It shall be noted that the use of RapidArc for treatments has the advantage that the treatment time is relatively short and the dose to the patient from monitoring with x-ray imaging might therefore be limited. This might serve as a rationale for using MLC-tracking with RapidArc compared to standard-IMRT or conformal radiotherapy.

In summary, this study confirms the capability of MLC-tracking to geometrically compensate for periodic target motion, giving considerably higher gamma index pass rates compared to not using motion compensation. The distance to adjacent MLC leaves was an important parameter to describe treatment plans suitability for MLC-tracking as plans with smaller distances showed better results. If used clinically, MLC-tracking has the potential to allow for decreased margins and reduced irradiation of healthy tissue, as well as an increased conformity when combined with intensity modulated treatment modalities such as RapidArc.

References

[1] T.Bortfeld, S.B.Jiang, E.Rietzel, Effects of motion on the total dose distribution. *Semin.Radiat.Oncol.* 14 (2004) 41-51

[2] L.Court, M.Wagar, R.Berbeco, A.Reisner, B.Winey, D.Schofield, D.Ionascu, A.M.Allen, R.Popple, T.Lingos, Evaluation of the interplay effect when using RapidArc to treat targets moving in the craniocaudal or right-left direction. *Med.Phys.* 37 (2010) 4-11.

[3] M.Falk, P.M.af Rosenschold, P.Keall, H.Cattell, B.C.Cho, P.Poulsen, S.Povzner, A.Sawant, J.Zimmerman, S.Korreman, Real-time dynamic MLC tracking for inversely optimized arc radiotherapy. *Radiother.Oncol.* 94 (2010) 218-223.

[4] A.Brahme, J.E.Roos, I.Lax, Solution of an integral equation encountered in rotation therapy. *Phys.Med. Biol.* 27 (1982) 1221-1229.

[5] Anders Brahme, Optimization of stationary and moving beam radiation therapy techniques, *Radiotherapy and Oncology*, 12 (1988) 129-140.

[6] T.Bortfeld, IMRT: a review and preview. *Phys.Med.Biol.* 51 (2006) R363-R379

[7] C.X.Yu, Intensity-modulated arc therapy with dynamic multileaf collimation: an alternative to tomotherapy. *Phys.Med.Biol.* 40 (1995) 1435-1449.

[8] C.X.Yu, X.A.Li, L.Ma, D.Chen, S.Naqvi, D.Shepard, M.Sarfaraz, T.W.Holmes, M.Suntharalingam, C.M.Mansfield, Clinical implementation of intensity-modulated arc therapy. *Int.J.Radiat.Oncol.Biol. Phys.* 53 (2002) 453-463.

[9] K.Otto, Volumetric modulated arc therapy: IMRT in a single gantry arc. *Med.Phys.* 35 (2008) 310-317.

[10] F. Kjær-Kristoffersen, L. Ohlhues, J. Medin, S. Korreman, RapidArc volumetric modulated therapy planning for prostate cancer patients, *Acta Oncol.*48 (2009) 227-232.

[11] E.J.Hall, Intensity-modulated radiation therapy, protons, and the risk of second cancers. *Int.J.Radiat. Oncol.Biol.Phys.* 65 (2006) 1-7

[12] W.Yang, L.Wang, J.Larner, P.Read, S.Benedict, K.Sheng, Tumor cell survival dependence on helical tomotherapy, continuous arc and segmented dose delivery. *Phys.Med.Biol.* 54 (2009) 6635-6643.

[13] S.Korreman, J.Medin, F.Kjaer-Kristoffersen, Dosimetric verification of RapidArc treatment delivery. *Acta Oncol.* 48 (2009) 185-191.

[14] A.Fogliata, A.Clivio, G.Nicolini, E.Vanetti, L.Cozzi, Intensity modulation with photons for benign intracranial tumours: a planning comparison of volumetric single arc, helical arc and fixed gantry techniques. *Radiother.Oncol.* 89 (2008) 254-262

[15] A.Fogliata, S.Yartsev, G.Nicolini, A.Clivio, E.Vanetti, R.Wyttenbach, G.Bauman, L.Cozzi, On the performances of Intensity Modulated Protons, RapidArc and Helical Tomotherapy for selected paediatric cases. *Radiat.Oncol.* 4 (2009) 2

[16] F.J.Lagerwaard, O.W.Meijer, E.A.van der Hoorn, W.F.Verbakel, B.J.Slotman, S.Senan, Volumetric modulated arc radiotherapy for vestibular schwannomas. *Int.J.Radiat.Oncol.Biol.Phys.* 74 (2009) 610-615.

[17] W.F.Verbakel, S.Senan, J.P.Cuijpers, B.J.Slotman, F.J.Lagerwaard, Rapid delivery of stereotactic radiotherapy for peripheral lung tumors using volumetric intensity-modulated arcs. *Radiother.Oncol.* 93 (2009) 122-124.

[18] W.F.Verbakel, J.P.Cuijpers, D.Hoffmans, M.Bieker, B.J.Slotman, S.Senan, Volumetric intensity-modulated arc therapy vs. conventional IMRT in head-and-neck cancer: a comparative planning and dosimetric study. *Int.J.Radiat.Oncol.Biol.Phys.* 74 (2009) 252-259.

[19] Q.J.Wu, S.Yoo, J.P.Kirkpatrick, D.Thongphiew, F.F.Yin, Volumetric arc intensity-modulated therapy for spine body radiotherapy: comparison with static intensity-modulated treatment. *Int.J.Radiat.Oncol.Biol.Phys.* 75 (2009) 1596-1604

[20] Varian Medical Systems, Eclipse algorithms reference guide. 2008, Varian Medical Systems, Inc.

[21] I.M.Gagne, W.Ansbacher, S.Zavgorodni, C.Popescu, W.A.Beckham, A Monte Carlo evaluation of RapidArc dose calculations for oropharynx radiotherapy. *Phys.Med.Biol.* 53 (2008) 7167-7185.

[22] L.R.Aarup, A.E.Nahum, C.Zacharatou, T.Juhler-Nottrup, T.Knoos, H.Nystrom, L.Specht, E.Wieslander, S.S.Korreman, The effect of different lung densities on the accuracy of various radiotherapy dose calculation methods: implications for tumour coverage. *Radiother.Oncol.* 91 (2009) 405-414

[23] C.M.Bragg, K.Wingate, J.Conway, Clinical implications of the anisotropic analytical algorithm for IMRT treatment planning and verification. *Radiother.Oncol.* 86 (2008) 276-284

[24] E Johansson (editor), Socialstyrelsen - Cancer i siffror 2009, 2009.

[25] R.D.Timmerman, B.D.Kavanagh, L.C.Cho, L.Papiez, L.Xing, Stereotactic body radiation therapy in multiple organ sites. *J.Clin.Oncol.* 25 (2007) 947-952.

[26] X.Qiao, O.Tullgren, I.Lax, F.Sirzen, R.Lewensohn, The role of radiotherapy in treatment of stage I non-small cell lung cancer. *Lung Cancer* 41 (2003) 1-11.

[27] Y.Seppenwoolde, H.Shirato, K.Kitamura, S.Shimizu, H.M.van, J.V.Lebesque, K.Miyasaka, Precise and real-time measurement of 3D tumor motion in lung due to breathing and heartbeat, measured during radiotherapy. *Int.J.Radiat.Oncol.Biol.Phys.* 53 (2002) 822-834.

[28] M.Guckenberger, T.Krieger, A.Richter, K.Baier, J.Wilbert, R.A.Sweeney, M.Flentje, Potential of image-guidance, gating and real-time tracking to improve accuracy in pulmonary stereotactic body radiotherapy. *Radiother.Oncol.* 91 (2009) 288-295.

[29] Court LE, M.Wagar, D.Ionascu, R.Berbeco, L.Chin, Management of the interplay effect when using dynamic MLC sequences to treat moving targets. *Med.Phys.* 35 (2008) 1926-1931.

[30] A.Sawant, R.Venkat, V.Srivastava, D.Carlson, S.Povzner, H.Cattell, P.Keall, Management of three-dimensional intrafraction motion through real-time DMLC tracking. *Med.Phys.* 35 (2008) 2050-2061.

[31] J.Zimmerman, S.Korreman, G.Persson, H.Cattell, M.Svatos, A.Sawant, R.Venkat, D.Carlson, P.Keall, DMLC motion tracking of moving targets for intensity modulated arc therapy treatment: a feasibility study. *Acta Oncol.* 48 (2009) 245-250.

[32] D.McQuaid, S.Webb, Target-tracking deliveries using conventional multileaf collimators planned with 4D direct-aperture optimization. *Phys.Med.Biol.* 53 (2008) 4013-4029.

[33] M.B.Tacke, S.Nill, A.Krauss, U.Oelfke, Real-time tumor tracking: automatic compensation of target motion using the Siemens 160 MLC. *Med.Phys.* 37 (2010) 753-761.

[34] B.Cho, P.R.Poulsen, A.Sloutsky, A.Sawant, P.J.Keall, First demonstration of combined kV/MV image-guided real-time dynamic multileaf-collimator target tracking. *Int.J.Radiat.Oncol.Biol.Phys.* 74 (2009) 859-867

[35] P.R.Poulsen, B.Cho, D.Ruan, A.Sawant, P.J.Keall, Dynamic multileaf collimator tracking of respiratory target motion based on a single kilovoltage imager during arc radiotherapy. *Int.J.Radiat.Oncol.Biol.Phys.* 77 (2010) 600-607.

[36] P.J.Keall, H.Cattell, D.Pokhrel, S.Dieterich, K.H.Wong, M.J.Murphy, S.S.Vedam, K.Wijesooriya, R.Mohan, Geometric accuracy of a real-time target tracking system with dynamic multileaf collimator tracking system. *Int.J.Radiat.Oncol.Biol.Phys.* 65 (2006) 1579-1584.

[37] A.Sawant, R.L.Smith, R.B.Venkat, L.Santanam, B.Cho, P.Poulsen, H.Cattell, L.J.Newell, P.Parikh, P.J.Keall, Toward submillimeter accuracy in the management of intrafraction motion: the integration of real-time internal position monitoring and multileaf collimator target tracking. *Int.J.Radiat.Oncol.Biol.Phys.* 74 (2009) 575-582.

[38] S.S.Vedam, P.J.Keall, A.Docef, D.A.Todor, V.R.Kini, R.Mohan, Predicting respiratory motion for four-dimensional radiotherapy. *Med.Phys.* 31 (2004) 2274-2283.

[39] D.A.Low, W.B.Harms, S.Mutic, J.A.Purdy, A technique for the quantitative evaluation of dose distributions. *Med.Phys.* 25 (1998) 656-661.

[40] D.A.Low, J.F.Dempsey, Evaluation of the gamma dose distribution comparison method. *Med.Phys.* 30 (2003) 2455-2464.

[41] D.Craft, P.Suss, T.Bortfeld, The tradeoff between treatment plan quality and required number of monitor units in intensity-modulated radiotherapy. *Int.J.Radiat.Oncol.Biol.Phys.* 67 (2007) 1596-1605

[42] M.Oliver, I.Gagne, C.Popescu, W.Ansbacher, W.A.Beckham, Analysis of RapidArc optimization strategies using objective function values and dose-volume histograms. *J.Appl.Clin.Med.Phys.* 11 (2010) 3114.

[43] Q.J.Wu, Z.Wang, J.P.Kirkpatrick, Z.Chang, J.J.Meyer, M.Lu, C.Huntzinger, F.F.Yin, Impact of collimator leaf width and treatment technique on stereotactic radiosurgery and radiotherapy plans for intra- and extracranial lesions. *Radiat.Oncol.* 4 (2009) 3.

[44] Z.Chang, Z.Wang, Q.J.Wu, H.Yan, J.Bowsher, J.Zhang, F.F.Yin, Dosimetric characteristics of novalis Tx system with high definition multileaf collimator. *Med.Phys.* 35 (2008) 4460-4463.

[45] Z.Wang, Z.Chang, Q.Wu, S.Zhou, C.Huntzinger, F.Yin, SU-GG-T-446: Dosimetric Characteristics of High Definition Multi-Leaf Collimator, *Med.Phys*. 35 (2008) 2827.

[46] J.A.Tanyi, P.A.Summers, C.L.McCracken, Y.Chen, L.C.Ku, M.Fuss, Implications of a high-definition multileaf collimator (HD-MLC) on treatment planning techniques for stereotactic body radiation therapy (SBRT): a planning study. *Radiat.Oncol.* 4 (2009) 22.

[47] T.Bortfeld, U.Oelfke, S.Nill, What is the optimum leaf width of a multileaf collimator? *Med.Phys.* 27 (2000) 2494-2502.

[48] R.Sadagopan, J.A.Bencomo, R.L.Martin, G.Nilsson, T.Matzen, P.A.Balter, Characterization and clinical evaluation of a novel IMRT quality assurance system. *J.Appl.Clin.Med.Phys.* 10 (2009) 2928.

[49] ScandiDos, Delta4 software user manual, 2009.

[50] Thomas Matzen, ScandiDos. Personal communication via Marianne Falk, November 3, 2010.

[51] M.Geurts, J.Gonzalez, P.Serrano-Ojeda, Longitudinal study using a diode phantom for helical tomotherapy IMRT QA. *Med.Phys.* 36 (2009) 4977-4983.

[52] J.L.Bedford, Y.K.Lee, P.Wai, C.P.South, A.P.Warrington, Evaluation of the Delta4 phantom for IMRT and VMAT verification. *Phys.Med.Biol.* 54 (2009) N167-N176.

Appendix

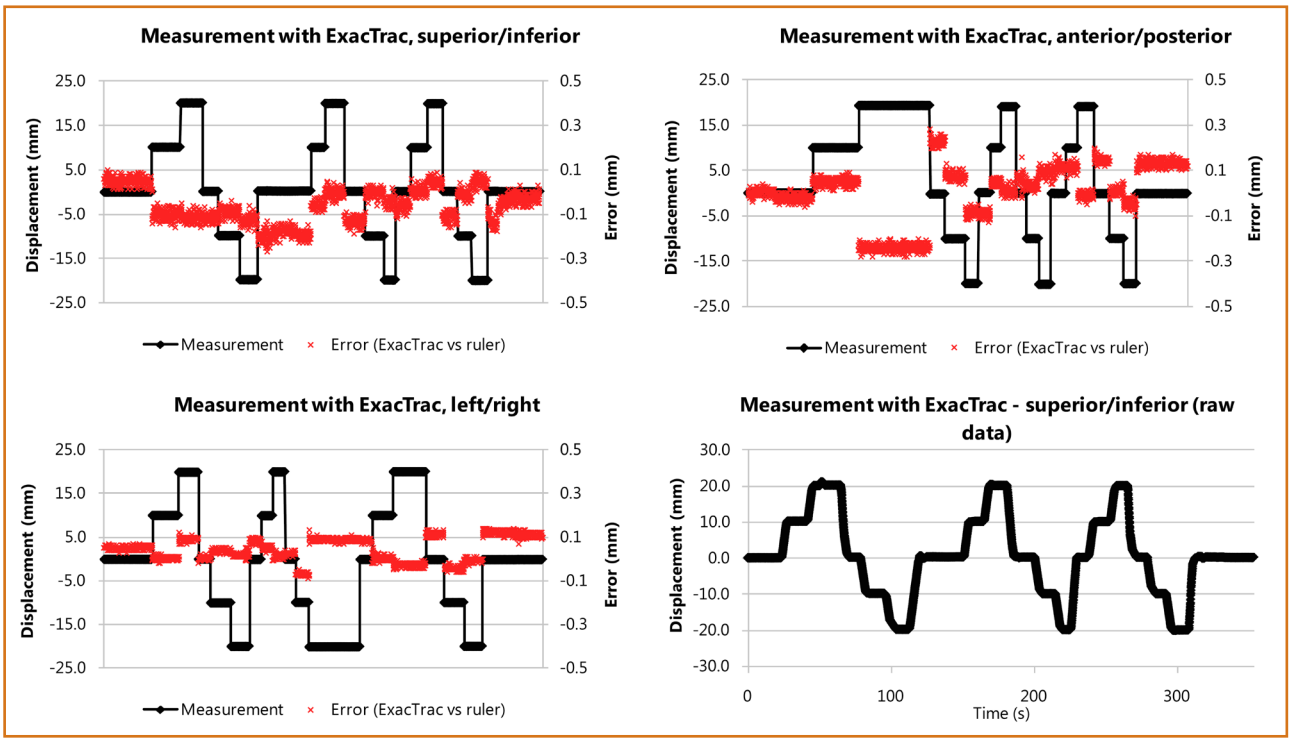

Figure 21. Measured position and error when compared to steel ruler with ExacTrac for three translations, as well as unfiltered data from one of the measurements (shown for completeness). In the top plots and bottom left plots, data collected when the couch was moved has been removed.

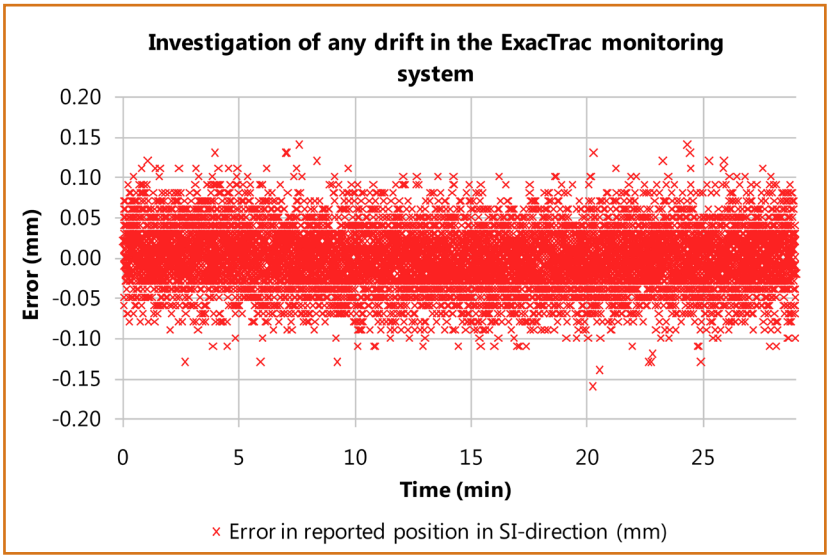

Figure 22. The error in measured poison from ExacTrac for approximately 30 minutes of measurements of a static target at isocenter.

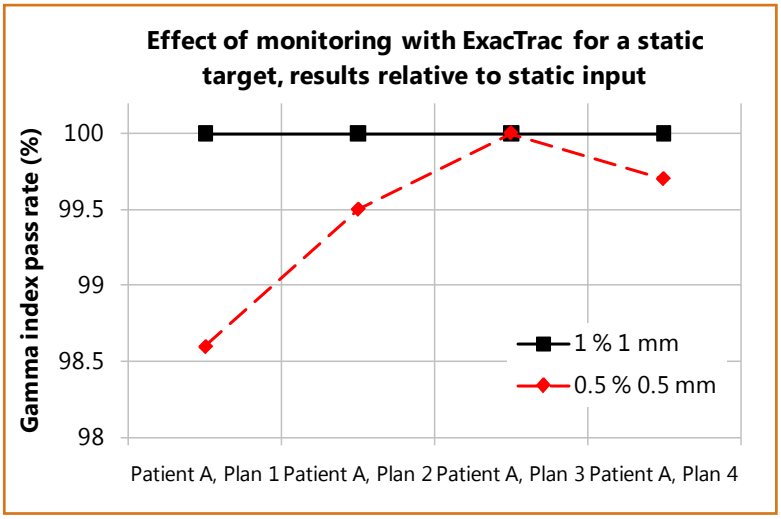

Figure 23. Effect of using the ExacTrac monitoring system for a static target, with a measurement with input from a data file for a static target used as reference.

Table 6. The geometric accuracy of MLC-tracking with the HDMLC for different assumed latencies and motion directions.

Assumed latency (ms)	Geometric accuracy (RMS, mm)	
	HDMLC	M-MLC
0 (i.e. no prediction)	1.906	1.862
200	0.355	0.382
210	0.316	0.371
220	0.320	0.364
230	0.342	0.346
240	0.413	0.405
250	0.457	0.478
260	0.477	0.468

Table 7. MLC-tracking results for treatment plans created for Patient A.

Plan id	Frequency of overdosage (>5%)	ALDw (cm)	Comparison with calculated dose distribution - Pass rate (3% 3 mm)			Comparison with measured dose distribution - Pass rate (2% 2 mm)	
			With MLC-tracking and moving target	No tracking, moving target	No tracking static target	With tracking, static measurement as reference	Without tracking, static measurement as reference
A01-HDMLC	36.9	0.581	86.45	91.8	100.0	84.1	71.3
A01-M-MLC	14.0	0.694	91.7	90.8	100.0	90.2	69.7
A02-HDMLC	46.5	0.754	84.1	91.5	98.6	83.0	69.4
A02-M-MLC	22.6	0.906	87.9	85.1	99.8	86.8	62.6
A03-HDMLC	46.2	0.786	83.5	77.4	99.0	79.1	59.2
A03-M-MLC	28.6	0.887	86.2	84.6	99.5	86.1	64.1
A04-HDMLC	60.4	0.841	81.4	87.3	96.9	78.8	68.5
A04-M-MLC	39.1	1.020	81.7	83.8	99.3	83.4	66.6
A05-HDMLC	0	-	98.9	93.6	100.0	98.5	73.0
A05-M-MLC	0	-	96.2	89.7	99.8	99.8	70.5
A06-HDMLC	0	-	95.9	94.1	100.0	97.5	73.9
A06-M-MLC	0	-	96.2	88.2	99.5	99.7	68.6
A07-HDMLC	0	-	96.9	87.0	99.3	98.6	69.6
A07-M-MLC	0	-	96.2	86.3	99.8	99.7	69.1
A08-HDMLC	0	-	95.0	87.7	98.9	95.9	67.2
A08-M-MLC	0	-	95.6	86.9	98.8	100.0	69.2
A09-HDMLC	0	0.343	100.0	93.0	100.0	98.5	72.6
A09-M-MLC	0	0.497	98.4	92.9	100.0	99.3	73.4
A10-HDMLC	13.6	0.694	88.8	90.7	99.0	87.4	67.7
A10-M-MLC	13.8	0.939	84.3	89.2	99.4	88.3	69.2
A11-HDMLC	0	0.300	92.1	89.0	98.1	99.0	68.6
A11-M-MLC	0.6	0.439	87.8	89.6	99.9	98.7	73.5

Table 8. MLC-tracking results for treatment plans created for patient B.

Plan id	Frequency of overdosage (>5%)	ALDw (cm)	Comparison with calculated dose distribution - Pass rate (3% 3 mm)			Comparison with measured dose distribution - Pass rate (2% 2 mm)	
			With MLC-tracking and moving target	No tracking, moving target	No tracking static target	With tracking, static measurement as reference	Without tracking, static measurement as reference
B01-HDMLC	31.8	0.452	89.8	83.2	100.0	88.2	47.8
B01-M-MLC	16.9	0.576	93.4	84.8	100.0	92.3	41.9
B02-HDMLC	51.9	0.578	86.4	84.3	99.5	87.3	50.8
B02-M-MLC	47.3	0.730	88.2	86.8	99.8	87.3	52.8
B03-HDMLC	54.0	0.602	85.2	82.1	99.3	86.2	53.2
B03-M-MLC	36.1	0.708	89.7	83.0	99.8	89.4	52.1
B04-HDMLC	41.1	0.586	88.3	81.5	99.3	87.1	47.7
B04-M-MLC	44.0	0.816	86.9	85.6	99.3	89.1	54.3
B05-HDMLC	0	-	95.6	89.2	99.5	99.0	48.1
B05-M-MLC	0	-	99.3	82.5	100.0	100.0	42.2
B06-HDMLC	0	-	95.5	81.2	98.5	98.8	42.1
B06-M-MLC	0	-	99.3	79.7	99.8	100.0	41.3
B07-HDMLC	0	-	94.9	82.6	98.5	97.8	45.0
B07-M-MLC	0	-	99.5	80.5	100.0	100.0	37.8
B08-HDMLC	0	-	95.8	86.9	99.0	98.3	43.5
B08-M-MLC	0	-	99.0	83.3	99.8	99.3	43.4
B09-HDMLC	0	0.325	99.3	84.8	100.0	99.5	48.0
B09-M-MLC	13.9	0.576	92.7	87.9	100.0	93.1	48.9
B10-HDMLC	57.0	0.578	85.2	80.6	99.5	86.3	51.2
B10-M-MLC	0	0.524	98.2	88.3	99.8	96.3	51.0
B11-HDMLC	0	0.319	95.8	83.9	99.8	97.4	49.7
B11-M-MLC	0	0.398	94.8	82.8	99.8	98.5	53.1

LUND UNIVERSITY

Faculty of Science